THE "STRESS AMPLIFICATION" MECHANISM FOR INTRAPLATE EARTHQUAKES APPLIED TO THE SOUTHEAST UNITED STATES

A THESIS

Presented to

The Faculty of the Division of Graduate

Studies and Research

By

Helmut Yung-An Hsiao

In Partial Fulfillment

of the Requirement for the Degree

Master of Science in Geophysical Sciences

Georgia Institute of Technology

August, 1977

THE "STRESS AMPLIFICATION" MECHANISM FOR INTRAPLATE EARTHQUAKES APPLIED TO THE SOUTHEAST UNITED STATES

Approved:

Dr. L. Timothy Long, Chairman

Dr. Robert P. Lowell

Dr. J. Marion Wampler

Date approved by Chairman

ACKNOWLEDGMENTS

I would like to express my sincere gratitide to Dr. L. T. Long, my thesis advisor, for his original ideal, guidance, patience, support and many helpful suggestions in analysis of the data throughout this entire work. Deep appreciation is extended toward Drs. J. M. Wampler, R. P. Lowell, members of my reading committee, for their critical review of this manuscript and their valuable suggestions. I also wish to thank Dr. J. Wang and Dr. C. Ueng for their criticism in the interpretation of the data.

Further recognition is given to Bill Volz, Scott Parks, and David Dunbar for their aid in solving some problems with regard to computer application. Special mention and thanks should also be given to George E. Marion and Stewart A. Guinn who gave generously and patiently of their time in order to produce a more fluent composition.

Finally, gratitude is extended to my parents and brothers and sisters for their love and encouragement during my endeavor.

This thesis, in part, was supported by the United States Nuclear Regulatory Commission, Grant Number AT(49-24)-0210, and by the National Science Foundation, Earth Science Section, NSF Grant Number DES75-15756.

TABLE OF CONTENTS

LIST OF TABLE

LIST OF ILLUSTRATIONS

LIST OF ILLUSTRATIONS
(Continued)

SUMMARY

As of this time seismic activity in the southeastern United States has not been related to mapped fault zones. The Great Smokey, Goat Rock, Modoc, Rome and other faults or fault zones with surface expression are typically paleozoic in age and appear to be inactive. Earthquakes that have been instrumentally located in the Southeast have not been related to these known faults.

Seismic activity in the southeastern United States is in close association with irregularities in crustal structure and hence with anomalous crustal rigidity or strength (Long, 1976). This close association suggests the hypothesis that crustal irregularities foster the concentration of stress in a deforming crust, and stress concentration may explain earthquakes in the southeastern United States.

In order to test this hypothesis, a mathematical stress modeling technique was developed to calculate the distribution of shear stress in inhomogeneous media. Shear stresses were initially calculated in three dimensions; however, excessive computer time prevented extensive use of three dimensional models. Consequently, the computations of stresses were largely restricted to two dimensional models. The two and three dimensional shear-stress computations were applied to models of the crustal structure near the Bowman, South Carolina seismic zone. These models were constrained by geologic, gravimetric and seismic refraction data. The results typically indicated higher stress accumulation in the thin high-velocity rigid portion of the model. Stresses in both the vertical and horizontal planes were calculated for the Bowman, South

Carolina, area. Results indicate that the planes of maximum shear stress are oriented from N to N45°W.

Free surface effects were investigated, and in general the interface between a material with high velocity and density and an overlying material with low velocity and density acts as free surface where the normal stress is close to zero.

CHAPTER I

INTRODUCTION

Earthquakes occur in regions of the earth's crust which are undergoing deformation. Energy is stored in the rock in the form of elastic stress. The stress which accompanies the readjustment of the earth's crust in response to tectonic forces may accumulate until it exceeds the yield strength of the rocks. Subsequently, fracture of fresh rock of movement along esixting faults may occur. The above mechanism is in essence, the elastic rebound theory, developed by Reid (1911) from data obtained after the great 1906 earthquake in San Francisco. The concept of the earthquake machanisms of the elastic rebound theory is based on two types of indirect observations:

1. Movement of surface rocks above the actual focal region
2. Behavior of rocks stressed in the laboratory under conditions similar to those within the earth.

Following fracture or movement along a fault, the opposite sides of the fault rebound to a position of equilibrium, and the energy is released in the form of heat, in the crushing of rock and in the vibration of elastic waves. The waves or vibrations which are generated at the moment of fracture produce the shaking which is experienced in an erathquake.

While Reid's theory is reasonable for shallow focus earthquakes, observations of frictional sliding in laboratory experiments (Jefferys, 1936) suggested that for deep-focus earthquakes, energy release due to fracture is unlikely. Orowan (1960), and Griggs and Baker (1969) proposed that a mechanism of thermal softening may be the mechanism for deep-focus earthquakes. In the

deep crust and in the upper mantle, the objections of Jeffreys (1936) to a mechanism based on frictional sliding may be valid. Although proposed mechamisms for shallow focus (i.e. frictional sliding) and deep-focus (i.e. thermal softening) earthquakes are different, the concept of a zone of relative weakness might tie both earthquake machanisms together.

If the fault surface and the dynamics of rupture could be observed directly, some relation between the earthquake mechanism and the dynamics of rupture might be found and explained by stick-slip or creep type movements. The most likely explanation for stick-slip movement during dry frictional sliding of brittle rocks at room temperature is an instability caused by sudden brittle fracture of locked regions on surfaces which may represent a zone of weakness between rocks. Motions within fault zones such as the San Andreas fault zone can take place suddenly to produce an earthquake. During such a sudden slip, the shear stress is released. The fault surfaces may then again become locked together until at some later time slip suddenly takes place. Shallow-focus earthquakes may represent stick-slip movement along old or newly formed faults. In such a situation, observed stress drops may represent a release of a small fraction of the stress supported by the rock surrounding the earthquake focus. Byerlee and Brace (1968) have shown that with a polished surface of a brittle material, the sliding will be stable if the normal stress is low, but unstable if the normal stress is high. However, Byerlee and Brace (1968) could not predict the stress at which the transition takes place. In the earth only a finite length of the fault moves during an earthquake, causing large stresses to be developed at the ends of the slipped section (Dieterich, 1969). Dieterich (1969) has shown that under these conditions the average shear-stress drop during sudden slip is about an order of magnitude lower than what

it would be if the fault were free to move unhindered by the surrounding material.

Byerlee and Brace (1972) have shown that there are a number of factors that affect the stability of sliding on a fault:

1. The presence of limestone, or porous tuff, or serpentine in gabbro and dunite will prevent the occurrence of stick-slip movement at all pressures.
2. The absence of stick-slip movement may be due to high temperature.
3. The absence of stick-slip movement may be caused by high fluid pore pressures within the fault zone.

Although unstable slip at high normal stress can explain stick-slip sliding on smooth surfaces the theory in its present form is only a qualitative one and is therefore not completely satisfactory. Ideally, one would like to be able to predict with some degree of certainty whether stick-slip or stable sliding will occur in any given situation.

If strain energy were accumulating in the earth's lithosphere from some tectonic process, then the superimposition of strain, could pretrigger an earthquake when some critical stress is reached. A possible example of a perturbation stress is stress associated with earth tides. Earth tides represent the largest pertubation strain in the earth with period less than one day. But the change in tidal stress with time is small compared to regional stress, and tidal stress may act as a perturbation which only affects the time of rupture.

Most of the above concepts apply to earthquakes which occur in seismic zones at the edges of plates or in established fault zones. But in the southeastern United States, which is in the interior of the North American Plate, no relation between the occurrence of earthquakes and known faults has been

found. Apparently, the known mechanisms of seismicity associated with plate edges or active established faults do not apply directly.

The Bowman, South Carolina, area (Mckee, 1974) may present a typical example of the above situation in the southeastern United States. Near Bowman the earthquake epicenters are located in a single epicentral zone and no faults are apparent at the surface. However, one unique feature of the epicentral zone near Bowman, Couth Carolina, is the association with a thinning in a rigid (i.e. anomalously high-velocity since the shear wave velocity is proportional to the square root of the modulus of rigidity) geologic unit of the crust.

Charleston similarly is characterized by an isolated epicentral zone and an association with rigid crustal units. A positive bouguer anomaly, which results from a large high-density basic intrustion as compared to the density of surrounding sedimentary rocks, exists near the epicentral zone of the 1886 Charleston earthquake. The historical data and some other recent data (Champion, 1975) strongly support an association between the seismicity and the high-density unit in the crust.

The geology of the CHRA (Clark Hill Reservior Area) is complex and combines more rigid gabbros, metadacites, mafic dikes, and amphibolites, with less rigid granite gneisses, schists, and phyllites (Long, et al. 1976). The irregular structures of those units might relate to the mechanism of CHRA earthquakes. The spectral characteristics of these quakes suggest that the stress drops are slightly high and that complete stress drop occurs during an earthquake (Marion, 1977).

In an attempt to explain the lack of obvious faults and the association of isolated epicentral zones with rigid crustal units, Long (Long, 1974; Long,

1976; Long and Hsiao, 1976) formulated an hypothesis for the occurrence of earthquakes in the southeastern United States, which says

> "Earthquakes occur in the southeastern United States because irregularities in crustal rigidity and crustal strength foster concentration of stress in a deforming crust. The geometries of the structures with anomalous rigidity and strength are determined primarily by the geometries of the major geologic units in the crust. Surficial sediments like the post-Cretaceous coastal plain sediments would have only a minimal secondary relation with earthquake occurrence. The positions of the crustal geologic units are determined by the contact zones between coherent crustal blocks or lateral irregularities within crustal block."

Older theories and hypotheses as to a possible mechanism which could account for accumulated stress are as follows:

1. Mechanical Forces:

   Ramberg (1967) suggested that some of the stresses which cause deformation in the crust are possibly generated by the following types of mechanical forces:

   (A) Force of Gravity: Expansion or contraction due to phase change results in a change in density which in turn gives rise to a buoyant or subsiding tendency. This effect produces an unstable mass distribution in the gravity field.

   (B) Stresses Transmitted Through The Surroundings to The Boundary of The System: The change or dynamic conditions in the surroundings affects the motion of the system as a unit.

   (C) Internal Stresses Due to Viscous Drag and Elastic Strain: Stable Mechanical equilibrium requires isotropic symmetry of the stress field. Since the crust is isotropic in composition and distribution, anisotropic stress does exist. Therefore, mechanical stability is disturbed by internal stresses such as viscous drag and elastic Strain.

Bollinger (1973) and Long (1975) have suggested that faulting in the southeastern United States is caused by the crust undergoing a gentle warping. Consequently, stress may be amplified or concentrated in old appalachian structures or brittle rock. The response to tectonic forces is evident in brittle rocks breaking, ductile rocks deforming, and elastic rocks bending. Fracture in brittle areas where stress is amplified should typically produce high stress-drop earthquakes (Bridges, 1975).

2. Influence of Fluid Intrusions:

   (A) Thermal Mechanism: In the CHRA, the thermal mechanism could play an important role in the stress accumulation. Cold water from the reservior may seep down into cracked rock and cool the warmer rocks a kilometer or so beneath the surface. As these rocks are cooled, they contract. This contraction could be the source of differential stress which eventually results in faulting (Lister, 1974).

   (B) It has been suggested that the water level may have a direct affect on the seismic activity associated with the Clark Hill Reservoir. When the water level rises above normal, activity typically becomes quiet. In this state, the extra vertical load increaces the confining pressure on the bottom. This enhances the vertical stress. But the net shear stress decreases, perhaps due to the existence of a larger horizontal stress. During unloading, the reverse occurs and earthquake activity increases (Talwani, 1976).

3. Temperature Effect:

   The temperature of the rocks near the surface has been decreasing

since the last intrusive or metamorphic event. As a result static friction is increased causing surfaces of low cohesion in the rock to stick and thus allowing stress to accumulate.

4. Tidal:

The solid earth tide is the longest single periodic strain in the earth. The tidal stress gradients are very small, being of the order of 10^{-10} bar/cm peak-to-peak (Knopoff, 1964). In the presence of a preexisting ambient stress field it is believed, in general, that forces associated with tides are too small to trigger activity. Knopoff (1964) further points out, based on correlations of small southern California earthquakes with tidal strains, that there is no detectable influence upon the times of earthquake occurrence by tides.

The temperature effect, although significant in deep earthquake regions, is negligible in this study since earthquakes in the southeastern United States are predominately shallow focus. The variations in fluid pressure and viscosity do play an important role in stress release. The Clark Hill Reservoir area is apparently affected by fluid level changes as pointed out by Talwani (1976). But in this study neither fluid nor viscous effects will be dealt with because of their complex nature. The tidal effect, as shown by Knopoff (1964) for shallow focus earthquakes in southern California, does not appear to be a causative mechanism and is probably not significant in the southeast.

This study will be based on Long's hypothesis, that southeastern United States earthquakes occur due to irregularities in crustal rigidity, crustal strength, and geometries of associated crustal blocks. The stress field was developed for the Bowman, South Carolina, epicenter area since gravity,

refraction and geologic data were available. These data provided information on geometry, crustal irregularities, and rigidity which were needed to define the model. Analysis of the stress field was achieved through mathematical modeling which depends on the theory of elasticity, to see if the model shows highest shear stresses in the observed epicentral zone. Such an association may allow one to find out where earthquakes are likely to occur in the southeastern United States.

CHAPTER II

MATHEMATICAL MODELING

Basic Equations

Almost all materials possess to a certain extent the property of elasticity. If the external forces producing deformation of any elastic material do not exceed the elastic limit, the deformation at least partly disappears with the removal of the forces. If the material completely recovers its original shape, it is said to be perfectly elastic; if it returns only partially to its original shape, it is partially elastic. The theory of elasticity is concerned with the strain experienced by a deformable material when subjected to stress. In this thesis, the assumption is made that solid media consist of particles which are sufficiently close-packed for the constitutive functions to be taken as continuous, isotropic, and differentiable. The materials are taken to be perfectly elastic. The possible existence of viscocity and plasticity of the material will not be considered.

The generalized Hooke's law relating stress to strain is (Timoshenko and Goodier, 1970)

$$\tau_{ij} = \lambda\theta\delta_{ij} + 2\mu e_{ij} \tag{1}$$

where

τ_{ij} is the stress tensor representing the stress in the ith direction on the plane perpendicular to the jth axis.

λ and μ are Lame's elastic parameters (μ is also called the shear modulus)

δ_{ij}: Kronnecker delta, $\delta_{ij}=0$. when $i=j$; $\delta_{ij}=1$, when $i=j$

e_{ij}: strain tensor, $e_{ij} = \frac{1}{2}(\frac{\partial U_i}{\partial x_j} + \frac{\partial U_j}{\partial x_i})$ (2)

Ui: the displacement in i direction and Ui=U1, U2, and U3 are the displacements in the 1, 2, and 3 directions respectively U_1=U1, U_2=U2, U_3=U3

θ :the dilation, $\theta = \frac{\partial U1}{\partial x_1} + \frac{\partial U2}{\partial x_2} + \frac{\partial U3}{\partial x_3}$ (3)

X_i: rectangular coordinate

From the equation of motion, we have

$$\frac{\partial^2 Ui}{\partial t^2} = \frac{\partial \tau_{ij}}{\partial x_j} + Fi \tag{4}$$

where Body Force Fi=o

We will consider the equilibrium condition for displacement Ui, so that the displacement Ui will be independent of time. Because the derivative with respect to time will be zero, equation (5) can be written,

$$\frac{\partial}{\partial x_j}\tau_{ij} = 0 = \frac{\partial^2 Ui}{\partial t^2} \tag{5}$$

where i,j=1,2,3

Substituting equations (1) and (2) into equation (5), one obtains,

$$0 = \lambda\frac{\partial^2 Uk}{\partial x_k \partial x_j} + \mu\frac{\partial^2 Ui}{\partial x_j \partial x_j} + \mu\frac{\partial^2 Uj}{\partial x_j \partial x_i} + \frac{\partial\lambda}{\partial x_j}\frac{\partial Uk}{\partial x_k} + \frac{\partial\mu}{\partial x_j}\frac{\partial Ui}{\partial x_j} + \frac{\partial\mu}{\partial x_j}\frac{\partial Uj}{\partial x_i} \tag{6}$$

where i,j,k=1,2,3

For the crust of the earth and the upper part of the mantle of the

earth, one has with sufficient approximation that $\lambda = \mu$ (which means that Poisson's ratio $\sigma \simeq \frac{1}{4}$). In this study, Lame's parameters μ, λ are considered to be a function of two dimension only.

$$\lambda = \lambda(x_1, x_3) \quad \text{and} \quad \mu = \mu(x_1, x_3) \tag{7}$$

From Ide (1936), we have

$$\lambda = \mu = \rho\beta^2 \tag{8}$$

Where β: S-wave velocity

ρ: density of material

(I) Three-Dimensional Model

On setting $\lambda = \mu$ and resolving equation (6) into three components, gives:

When i=1

$$0 = 3\frac{\partial^2 U1}{\partial x_1^2} + 2\frac{\partial^2 U2}{\partial x_1 \partial x_2} + 2\frac{\partial^2 U3}{\partial x_1 \partial x_3} + \frac{\partial^2 U1}{\partial x_2^2} + \frac{\partial^2 U1}{\partial x_3^2} + \frac{1}{\lambda}\{\frac{\partial \lambda}{\partial x_1}(3\frac{\partial U1}{\partial x_1} + \frac{\partial U2}{\partial x_2} + \frac{\partial U3}{\partial x_3}) + \frac{\partial \lambda}{\partial x_3}(\frac{\partial U1}{\partial x_3} + \frac{\partial U3}{\partial x_1})\} \tag{9}$$

When i=2

$$0 = 3\frac{\partial^2 U2}{\partial x_2^2} + 2\frac{\partial^2 U1}{\partial x_1 \partial x_2} + 2\frac{\partial^2 U3}{\partial x_2 \partial x_3} + \frac{\partial^2 U2}{\partial x_1^2} + \frac{\partial^2 U2}{\partial x_3^2} + \frac{1}{\lambda}\{\frac{\partial \lambda}{\partial x_1}(\frac{\partial U2}{\partial x_1} + \frac{\partial U1}{\partial x_2}) + \frac{\partial \lambda}{\partial x_3}(\frac{\partial U2}{\partial x_3} + \frac{\partial U3}{\partial x_2})\} \tag{10}$$

When i=3

$$0 = 3\frac{\partial^2 U3}{\partial x_3^2} + 2\frac{\partial^2 U2}{\partial x_2 \partial x_3} + 2\frac{\partial^2 U1}{\partial x_1 \partial x_3} + \frac{\partial^2 U3}{\partial x_1^2} + \frac{\partial^2 U3}{\partial x_2^2} + \frac{1}{\lambda}\{\frac{\partial \lambda}{\partial x_3}(3\frac{\partial U3}{\partial x_3} + \frac{\partial U2}{\partial x_2} + \frac{\partial U1}{\partial x_1}) + \frac{\partial \lambda}{\partial x_1}(\frac{\partial U3}{\partial x_1} + \frac{\partial U1}{\partial x_3})\} \tag{11}$$

Second order finite difference equations are used to approximate the partial derivatives at grid points. The finite difference derivatives of the displacement Ui, which are the central differences at the grid point $(x_1, x_2, x_3,)=(x,y,z)$ take the form,

$$\frac{\partial U1}{\partial x} = (U1_{x+1\ y\ z} - U1_{x-1\ y\ z})/2\Delta x \tag{12}$$

$$\frac{\partial^2 U1}{\partial x^2} = (U1_{x+1\ y\ z} - 2U1_{x\ y\ z} + U1_{x-1\ y\ z})/(\Delta x)^2 \tag{13}$$

$$\frac{\partial^2 U1}{\partial x \partial y} = (U1_{x+1\ y+1\ z} - U1_{x+1\ y-1\ z} - U1_{x-1\ y+1\ z} + U1_{x-1\ y-1\ z})/4(\Delta x)(\Delta y) \tag{14}$$

Equations (12,13,14) are substituted into equations (9,10,11) for numerical evaluation of displacement at each grid point. The part that discribes homogeneous media consists only of the first five terms of equations (9,10,11).

On solving for the displacements at the central point (x,y,z), the finite difference expressions for the displacements in homogeneous media become

$$\begin{aligned} 10U1_{x\ y\ z} = {} & 3(U1_{x-1\ y\ z} + U1_{x+1\ y\ z}) + U1_{x\ y+1\ z} + U1_{x\ y-1\ z} + U1_{x\ y\ z-1} \\ & + U1_{x\ y\ z+1} + \frac{1}{2}(U2_{x+1\ y+1\ z} - U2_{x-1\ y+1\ z} - U2_{x+1\ y-1\ z} + U2_{x-1\ y-1\ z} \\ & + U3_{x+1\ y\ z+1} - U3_{x-1\ y\ z+1} - U3_{x+1\ y\ z-1} + U3_{x-1\ y\ z-1}) \end{aligned} \tag{15}$$

$$\begin{aligned} 10U2_{x\ y\ z} = {} & 3(U2_{x\ y-1\ z} + U2_{x\ y+1\ z}) + U2_{x-1\ y\ z} + U2_{x+1\ y\ z} + U2_{x\ y\ z-1} \\ & + U2_{x\ y\ z+1} + \frac{1}{2}(U1_{x+1\ y+1\ z} - U1_{X-1\ y+1\ z} - U1_{x+1\ y-1\ z} \\ & + U1_{x-1\ y-1\ z} + U3_{x\ y+1\ z+1} - U3_{x\ y-1\ z+1} - U3_{x\ y+1\ z-1} \\ & + U3_{x\ y-1\ z-1}) \end{aligned} \tag{16}$$

$$10U3_{x\ y\ z} = 3(U3_{x\ y\ z+1} + U3_{x\ y\ z-1}) + U3_{x+1\ y\ z} + U3_{x-1\ y\ z} + U3_{x\ y+1\ z}$$
$$+ U3_{x\ y-1\ z} + \frac{1}{2}(U1_{x+1\ y\ z+1} - U1_{x-1\ y\ z+1} - U1_{x+1\ y\ z-1}$$
$$+ U1_{x-1\ y\ z-1} + U2_{x\ y+1\ z+1} - U2_{x\ y-1\ y+1} - U2_{x\ y+1\ z-1}$$
$$+ U2_{x\ y-1\ z-1}) \qquad (17)$$

The models considered in this thesis consists of two or three homogeneous regions of different rigidity. The boundaries between the homogeneous regions are formulated by considering the boundaries as sharp inhomogeneities. In the computations such boundaries or inhomogeneities can be accounted for by adding appropriate additional terms to equations (15,16,17). The terms are derived by substituting equations (12,13,14) into the part of equations (9,10,11) which represent inhomogeneous media.

The effects of the inhomogeneous media can be calculated from the following equations:

$$AKi = \frac{1}{\lambda}\left(\frac{\partial\lambda}{\partial x_i \partial x_i}\right) \simeq \frac{1}{\lambda}\left(\frac{\Delta\lambda}{2\Delta x_i}\ \frac{1}{2\Delta x_i}\right)$$
$$= \pm\frac{1}{4}\ \frac{1}{(\Delta x_i)^2}\ \frac{\Delta\lambda}{\lambda} = \pm\frac{1}{4}\ \frac{1}{(\Delta x_i)^2}\ \left(\frac{\rho_1\beta_1^2 - \rho_3\beta_3^2}{\rho_i\beta_i^2}\right)$$
$$= \pm\frac{1}{4}\ \frac{1}{(\Delta x_i)^2}\ \left(\frac{\rho_1\beta_1^2 - \rho_3\beta_3^2}{\rho_i\beta_i^2}\right) \qquad (18)$$

In the calculation of the homogeneous terms the $\left(\frac{1}{\Delta X_i^2}\right)$ terms were canceled. Therefore the $\left(\frac{1}{\Delta X_1^2}\right)$ term in equation (18) must be canceled, leaving

$$AK1 \simeq \pm\frac{1}{4}\left(\frac{\rho_1\alpha_1^2 - \rho_3\alpha_3^2}{\rho_1\alpha_1^2}\right) \qquad (19)$$

$$AK3 \simeq \pm\frac{1}{4}\left(\frac{\rho_1\alpha_1^2 - \rho_3\alpha_3^2}{\rho_3\alpha_3^2}\right) \tag{20}$$

The signs of the AK depends on the sign of the gradient of the Lame's elastic parameters. (i.e. $\frac{\partial\lambda}{\partial x} \simeq \frac{\Delta\lambda(1) - \Delta\lambda(2)}{\Delta x(1) - \Delta x(2)}$) (21)

Combining the homogeneous and inhomogeneous terms and establishing boundary conditions, according to the geology or other geophysical information, one can assume an initial displacement and use the differential equations and the methods of successive approximation to calculate the displacement of each grid point with respect to the surrounding points. Once a sufficiently stable solution is obtained one can use equation (1) to calculate the components of the stress acting on the six sides of a cubic element (assuming that each point is an infinitesmal cubic element). The three normal stresses are τ_{11}, τ_{22}, τ_{33} and the six shearing stress are $\tau_{12}=\tau_{21}$, $\tau_{23}=\tau_{32}$, and $\tau_{31}=\tau_{13}$. Once the stress components for the three coordinate planes are known, one can determine the directions and magnitudes of the principal stresses by using the property that the principal stresses are perpendicular to the planes on which they act. Let l,m,n be the direction cosines of a principal plane and S the magnitude of the principal stress acting on this plane. Then the components of this stress are

$$X = Sl \ , \quad Y = Sm \ , \quad Z = Sn \tag{22}$$

From Timoshenko and Goodier (1970), the relation between the components of stress at each point and the principal stresses are given as:

$$S^3 - I_1S^2 + I_2S - I_3 = 0 \tag{23}$$

Where

$$I_1 = \tau_{11} + \tau_{22} + \tau_{33} \tag{24}$$

$$I_2 = \tau_{11}\tau_{22} + \tau_{22}\tau_{33} + \tau_{33}\tau_{11} - \tau_{12}^2 - \tau_{23}^2 - \tau_{31}^2 \tag{25}$$

$$I_3 = \tau_{12}\tau_{22}\tau_{33} + 2\tau_{12}\tau_{23}\tau_{31} - \tau_{11}\tau_{23}^2 - \tau_{22}\tau_{13}^2 - \tau_{33}\tau_{12}^2 \tag{26}$$

The three roots of equation (23) give the values of the three principal stresses S1, S2, S3. Then, writing

$$X = S - \frac{I_1}{3} \tag{27}$$

Which is

$$S = X - \frac{I_1}{3} \tag{28}$$

Substituting equation (28) into equation (23) and after rearranging terms, one obtains:

$$X^3 + aX + b = 0 \tag{29}$$

Where

$$a = I_2 - \frac{1}{3} I_1^2 \tag{30}$$

and

$$b = -\frac{1}{27}(2I_1^3 - 9I_1I_2 + 27I_3) \tag{31}$$

The roots for equation (23) are

$$S_1 = \frac{I_1}{3} + 2\sqrt{-a/3}\ \cos(\phi/3) \tag{32}$$

$$S_2 = \frac{I_1}{3} + 2\sqrt{-a/3}\ \cos\{(\phi+2\pi)/3\} \tag{33}$$

$$S_3 = \frac{I_1}{3} + 2\sqrt{-a/3}\ \cos\{(\phi+4\pi)/3\} \tag{34}$$

in which

$$\phi = \cos^{-1}\{(-b/2\sqrt{-a^3/27}\} \tag{35}$$

The maximum shearing stresses are

$$\tau_1 = \pm\frac{1}{2}(S_1-S_2) \quad , \quad \tau_2 = \pm\frac{1}{2}(S_1-S_3) \quad , \quad \tau_3 = \pm\frac{1}{2}(S_2-S_3) \tag{36}$$

This shows that the maximum shearing stress acts on the plane bisecting the angle between the largest and the smallest principal stresses and is equal to half the difference between these two principal stresses. Equations (22,23,24) are the magnitudes of the principal stresses.

The directions of the principal stresses can be calculated by

$$\begin{bmatrix} \tau_{11} & \tau_{12} & \tau_{13} \\ \tau_{21} & \tau_{22} & \tau_{23} \\ \tau_{31} & \tau_{32} & \tau_{33} \end{bmatrix} \begin{bmatrix} l(i) \\ m(i) \\ n(i) \end{bmatrix} = S(i) \begin{bmatrix} l(i) \\ m(i) \\ n(i) \end{bmatrix} \tag{37}$$

Where l(i), m(i), n(i) are the three components of the ith principal stress, i=1,2,3, and $\tau_{12}=\tau_{21}$, $\tau_{23}=\tau_{32}$, $\tau_{31}=\tau_{13}$.

Then, from equation (37)

$$\begin{aligned} (\tau_{11} - S_i)l(i) + \tau_{12}\, m(i) + \tau_{13}\, n(i) &= 0 \\ \tau_{21}\, l(i) + (\tau_{22} - S_i)m(i) + \tau_{23}\, n(i) &= 0 \\ \tau_{31}\, l(i) + \tau_{23}\, m(i) + (\tau_{33} - S_i)n(i) &= 0 \end{aligned} \tag{38}$$

with the additional requirement that

$$l^2(i) + m^2(i) + n^2(i) = 1 \tag{39}$$

From the above equations with 3 unknown variables, giving three solutions as follows:

$$l(i) = \left| \sqrt{\frac{1}{1 + G^2 + F^2}} \right| \tag{40}$$

$$m(i) = G(i) \cdot l(i) \tag{41}$$

$$n(i) = F(i) \cdot l(i) \tag{42}$$

Where

$$G(i) = \frac{\tau_{11}\tau_{23} - \tau_{23}S_i - \tau_{12}\tau_{13}}{\tau_{23}\tau_{13} - \tau_{13}S_i - \tau_{12}\tau_{23}} \tag{43}$$

$$F(i) = \frac{\tau_{12}\tau_{23} - \tau_{13}(\tau_{22} - S_i)}{(\tau_{33} - S_i)(\tau_{22} - S_i) - \tau_{23}^2} \tag{44}$$

Therefore, $S_i \begin{bmatrix} l(i) \\ m(i) \\ n(i) \end{bmatrix}$, i=1,2,3 are the components of the three principal stresses.

i.e. S_1 l(i) is the component of the first principal stress on the x axis of the original coordinate system.

One can express V the strain energy per unit volume as a function of the stress components.

$$V = \frac{1}{2E}(\tau_{11}^2 + \tau_{22}^2 + \tau_{33}^2) + \frac{1}{2\mu}(\tau_{12}^2 + \tau_{23}^2 + \tau_{31}^2) - \frac{\sigma}{E}(\tau_{11}\tau_{22} + \tau_{22}\tau_{33} + \tau_{33}\tau_{11}) \tag{45}$$

where σ: Poisson ratio when

$$\mu = \frac{E}{2(1+\sigma)} = \frac{2E}{5} \tag{46}$$

$$\frac{\sigma}{E} = \frac{1}{10\mu} \tag{47}$$

Rearranging equation (45), gives:

$$V = \frac{1}{10\mu}\{2(\tau_{11}^2 + \tau_{22}^2 + \tau_{33}^2) - (\tau_{11}\tau_{22} + \tau_{22}\tau_{33} + \tau_{33}\tau_{11}) + 5(\tau_{12}^2 + \tau_{23}^2 + \tau_{31}^2)\} \tag{48}$$

The magnitude and direction of the principal stresses and maximum shearing stresses are calculated at each point by using the corresponding displacements. Finally, the total strain energy per unit volume at each

point is calculated from the respective values of stresses using the above parameters. One can find the zones of greatest shear stress and hence the most probable areas for earthquake occurrence. Because of the complexity of boundary conditions in setting up a realistic three-dimensional model, only one model was solved in three-dimension. This model was the Bowman, South Carolina crustal structure subjected to vertical uplift on one end. In this study most crustal structures were reduced to simpler two-dimensional models.

(II) Two-Dimensional Models

The two-dimensional models allow one to calculate stress distribution for a wider variety of models using a greater variety of boundary conditions than would be possible with the more complex three-dimensional models in the same amount of computer time. Also, one will have enough computer time to calculate many models in two-dimensions without considering the computer expenses.

As in the three-dimensional model, the Lamé parameters (μ,λ) of the two-dimensional models are considered to be a functions of x_1 and X_2. Then, the equation (7) becomes,

$$\lambda = \lambda(X_1,X_2) \quad , \qquad \mu = \mu(X_1,X_2) \tag{49}$$

Setting $\lambda=\mu$ and resolving equation (6) into two-dimensions, gives,

$$\text{When } i = 1, \quad 0 = 3\frac{\partial^2 U1}{\partial x_1^2} + 2\frac{\partial^2 U2}{\partial x_1 \partial x_2} + \frac{\partial^2 U1}{\partial x_2^2} + \frac{1}{\lambda}\{\frac{\partial \lambda}{\partial x_1}(3\frac{\partial U1}{\partial x_1} + \frac{\partial U2}{\partial x_2}) + \frac{\partial \lambda}{\partial x_2}(\frac{\partial U1}{\partial x_2} + \frac{\partial U2}{\partial x_1})\} \tag{50}$$

When i = 2

$$0 = 3\frac{\partial^2 U2}{\partial x_2^2} + 2\frac{\partial^2 U1}{\partial x_2 \partial x_1} + \frac{\partial^2 U2}{\partial x_1^2} + \frac{1}{\lambda}\{\frac{\partial \lambda}{\partial x_1}(\frac{\partial U1}{\partial x_2} + \frac{\partial U2}{\partial x_1}) + \frac{\partial \lambda}{\partial x_2}(\frac{\partial U1}{\partial x_1} + 3\frac{\partial U2}{\partial x_2})\} \tag{51}$$

Homogeneous Computations

Using the finite difference equations (12,13,14), the homogeneous parts of equations (50,51) become

$$0 = \frac{3}{(\Delta x)^2}(U1_{x+1\ y} - 2U1_{x\ y} + U1_{x-1\ y}) + \frac{2}{4(\Delta x)(\Delta y)}(U2_{x+1\ y+1} - U2_{x+1\ y-1} - U2_{x-1\ y+1} + U2_{x-1\ y-1}) + \frac{1}{(\Delta y)^2}(U1_{x\ y+1} - 2U1_{x\ y} + U1_{x\ y-1}) \tag{52}$$

$$0 = \frac{3}{(\Delta y)^2}(U2_{x\ y+1} - 2U2_{x\ y} + U2_{x\ y-1}) + \frac{2}{4(\Delta x)(\Delta y)}(U1_{x+1\ y+1} - U1_{x+1\ y-1} - U1_{x-1\ y+1} + U1_{x-1\ y-1}) + \frac{1}{(\Delta x)^2}(U2_{x+1\ y} - U2_{x\ y} + U2_{x-1.y}) \tag{53}$$

Where $\Delta x = \Delta y$ (54)

Rearranging equations (52,53), the displacements of each grid point of the homogeneous interior part, is

$$U1_{x\ y} = \{3(U1_{x+1\ y} + U1_{x-1\ y}) + U1_{x\ y+1} + U1_{x\ y-1} + \frac{1}{2}(U2_{x+1\ y+1} - U2_{x+1\ y-1} - U2_{x-1\ y+1} + U2_{x-1\ y-1})\}/8 \tag{55}$$

$$U2_{x\ y} = \{3(U2_{x\ y+1} + U2_{x\ y-1}) + U2_{x+1\ y} + U2_{x-1\ y}) + \frac{1}{2}(U1_{x+1\ y+1} - U1_{x+1\ y-1} - U1_{x-1\ y+1} + U1_{x-1\ y-1})\}/8 \tag{56}$$

Inhomogeneous Computations

The two-dimensional inhomogeneous factors can be calculated approximately from equation (18) to be

$$Ak1 \simeq \pm\frac{1}{4}\left(\frac{\rho_1\alpha_1^2 - \rho_2\alpha_2^2}{\rho_1\alpha_1^2}\right) \tag{57}$$

$$Ak2 \simeq \pm\frac{1}{4}\left(\frac{\rho_1\alpha_1^2 - \rho_2\alpha_2^2}{\rho_2\alpha_2^2}\right) \tag{58}$$

Stresses Computations

The three stress components (from equation (1)) can be presented in the forms:

$$\tau_{11} = T(1) = \mu\{3(U1_{x+1\ y} - U1_{x-1\ y}) + U2_{x\ y+1} - U2_{x\ y-1}\}/2\Delta x \tag{59}$$

$$\tau_{22} = T(2) = \mu\{3(U2_{x\ y+1} - U2_{x\ y-1}) + U1_{x+1\ y} - U1_{x-1\ y}\}/2\Delta x \tag{60}$$

$$\tau_{21} = T(3) = \mu(U1_{x\ y+1} - U1_{x\ y-1} + U2_{x+1\ y} - U2_{x-1\ y})/2\Delta x \tag{61}$$

$$\tau_{21} = \tau_{12} \tag{62}$$

From "Theory of Elasticity" (Timoshenko and Goodier, (1970), the principal stresses, T(4) and T(5), are obtained from

$$T(4) = A+B \tag{63}$$

and $$T(5) = A-B \tag{64}$$

The maximum shearing stress is given as

$$T(6) = \frac{T(4) - T(5)}{2} = B \tag{65}$$

where

$$A = \frac{1}{2}(T(1) + T(2)) \tag{66}$$

$$B = \sqrt{\{(T(1) - T(2))/2\}^2 + T(3)^2} \tag{67}$$

The angle between the axis of the principal stress and the coordinate axis is

$$\Phi = \frac{1}{2} \tan^{-1}\{2T(3)/(T(1) - T(2))\} \tag{68}$$

The strain energy per unit volume is

$$V_0 = \{2(T(1)^2 + T(2)^2) - T(1)\cdot T(2) + 5T(3)^2\}/10\mu \tag{69}$$

In this manner, all necessary features of the stress distribution at a point can be obtained if only the three stress components T(1), T(2), T(3) are known.

(III) Boundary Conditions and Models

The Bowman, South Carolina, earthquakes are used as an example to test the hypothesis. Bowman is located at 34.46° N, 80.58° W near Orangeburg, South Carolina. An earthquake with a maximum intensity of IV occurred near Bowman at 12:53 GMT on May 19, 1971. Before that time no

earthquakes had been reported within a radius of 50 Km from the epicentral area. Three additional earthquakes of intensity III to V and their aftershocks occurred within eighteen months. From more than three hundred points of gravity data in the vicinity of Bowman, Mckee (1974) has suggested that a high-density basement structure trending NE-SW underlies the epicentral area. Magnetic data imply a higher magnetic susceptibility in the structure than in the surrounding basement materials. The gravity contour lines suggest a structure shape as shown in Figure 1. Two and three-dimensional models of the structure were developed to study its influence on an applied stress field and the possibility for stress amplification.

A Three-Dimensional Model

By using Mckee's (1974) theoretical gravity modeling of a crustal structure near Bowman, South Carolina and applying the concept of stress amplification (Long, 1974), a three-dimensional model for the computation of stress can be developed as shown in Figure 2. Because of the symmetry of the structure, computation of stress in only one quadrant of the structure was necessary as shown in Figure 2. For simplification, the same density, 3.0 gm/cm^3, was used for the two media. The velocity of medium I is 6 km/sec and of medium II is 5 km/sec.

On the top, the boundary condition was a free surface. On the bottom, differential vertical movement between two crustal blocks was simulated with a hydrostatic force with a cosine amplitude function and bouyant restoring force. The two ends and two sides were fixed in the horizontal direction but were free to move vertically. The concepts and

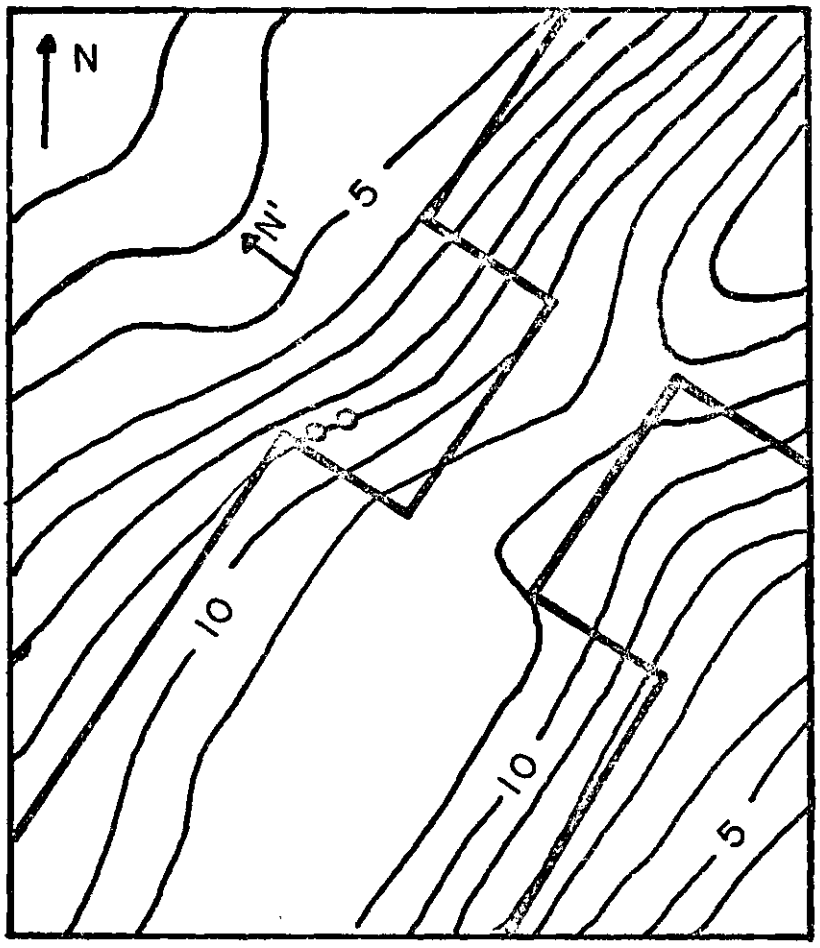

Figure 1. Simple Bouguer Gravity Map of Bowman, South Carolina, Area (after Mckee, 1974) with Horizontal Model and Microearthquake Epicenters Superimposed.

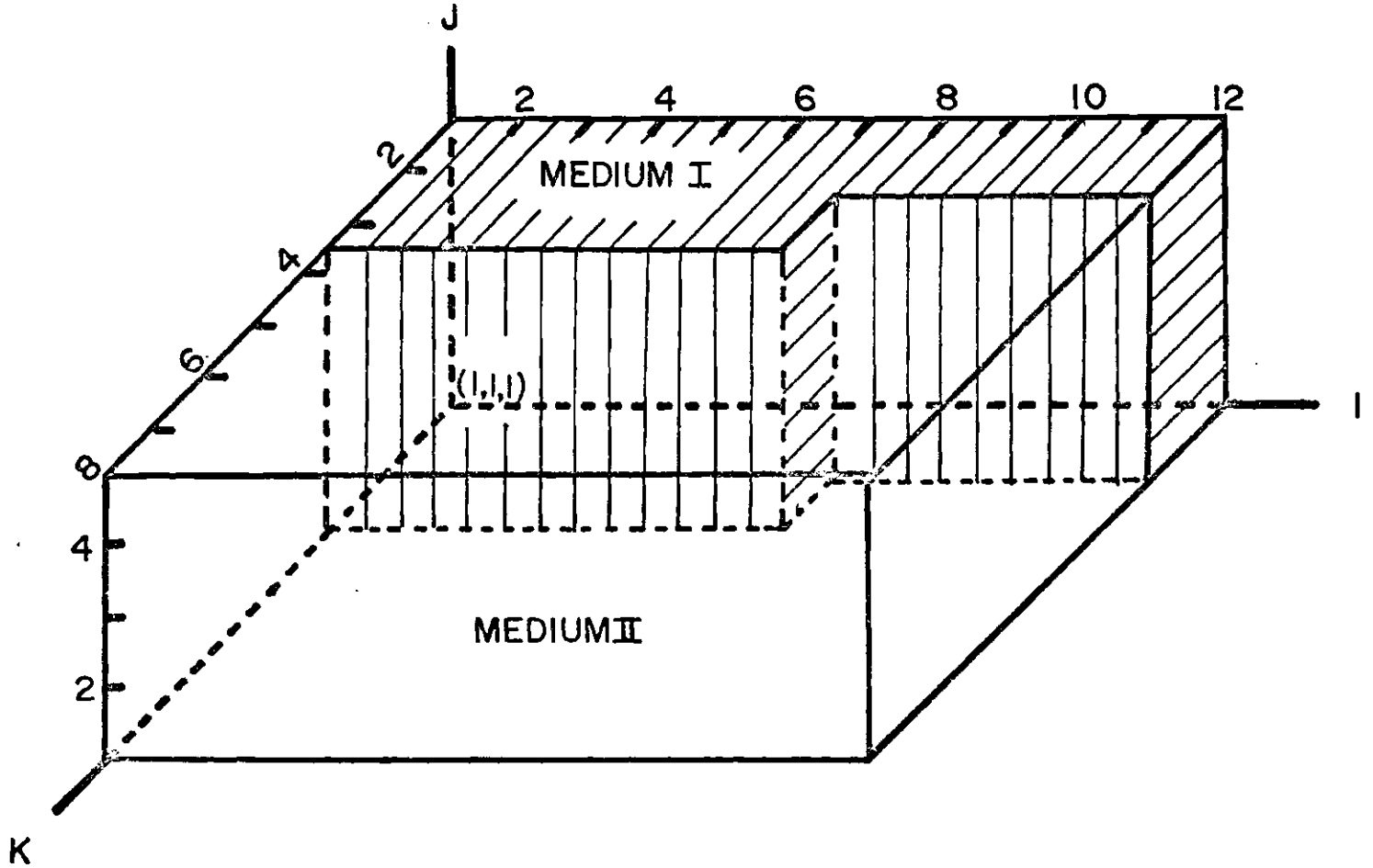

Figure 2. Three-Dimensional Stress Model of Bowman Area

computations of the boundary conditions in the three-dimensional model are similar to those of the two-dimensional models, but algebraically more complex. Therefore, details in the three-dimensional model are not given since they follow directly from the methods applied to the two-dimensional models.

B Two-Dimensional Vertical Model

A two-dimensional model was computed in the vertical plane with the same boundary conditions as were used in the three-dimensional model (see Figure 3). Some of the detailed gravity data near Bowman (Mckee, 1974) can be interpreted as implying the existence of a fault or change in depth to the basement.

Woollard's (1957) refraction data provided velocities of 2.4 km/sec for medium I and 6.9 km/sec for medium II. The density-velocity curve of Nafe and Drake (1959) gave respective densities of 2.1 gm/cm^3 and 3.0 gm/cm^3 for mediums I and II. Using the above densities along with gravity data, Mckee (1974) estimated the depth to basement at 0.5 km. The model then consists of a high-velocity high-density vertical intrusive overlain by the coastal plain sediments as shown in Figure 3. This model was also utilized to evaluate the significance of the coastal plain cover in earthquakes and stress accumulations.

Computation for Homogeneous media

From size in Figure 3 one knows the range of coordinates x,y in equations (55,56) are limited in dimensions to $2 \leq x \leq 20$ and $2 \leq y \leq 5$.

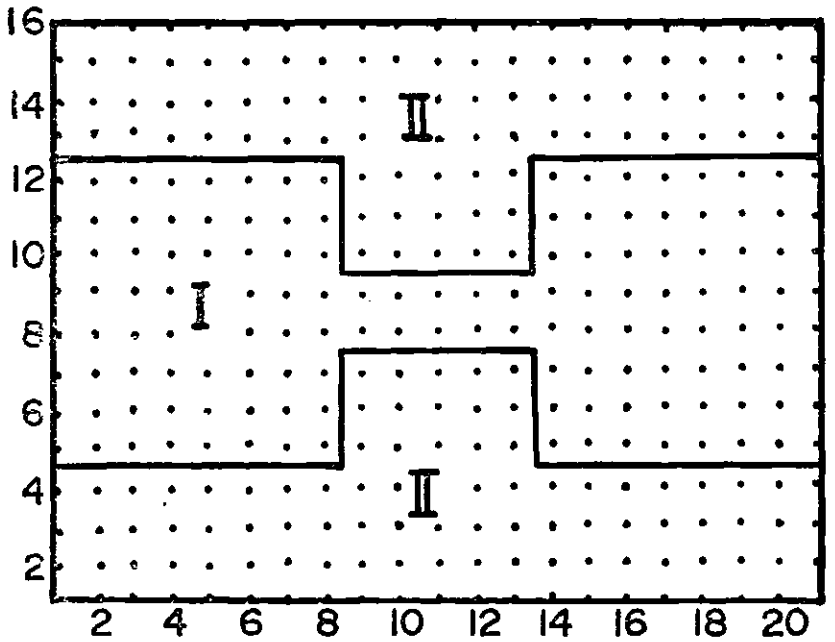

Figure 4. Two-Dimensional Horizontal Stress Model of Bowman, South Carolina, Area.

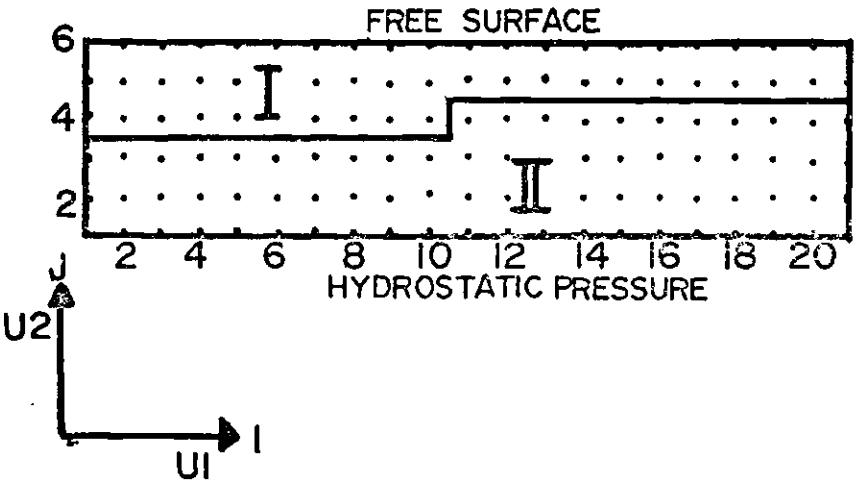

Figure 3. Two-Dimensional Vertical Stress Model of Bowman, South Carolina, Area.

Computation for Inhomogeneity

Equations for the computations at boundaries between layers will be presented in this section. In the computation the inhomogeneous terms are added to the homogeneous equations. From the above and Table 1, one obtains velocities and densities for using in the equations of

$$\alpha_2 = 6.9 \text{ km/sec} \tag{70}$$

$$\alpha_1 = 2.4 \text{ km/sec} \tag{71}$$

$$\rho_2 = 3.0 \text{ g/cm} \tag{72}$$

$$\rho_1 = 2.1 \text{ g/cm} \tag{73}$$

Substituting equations (70-73) into equations (57,58), one has

$$Ak2 = \pm 0.2288 \tag{74}$$

$$Ak1 = \pm 2.702 \tag{75}$$

The signs of the AKi depends on the sign of the gradient of the Lame elastic parameters.

The inhomogeneous parts of the equations (50,51) become

$$IU1_{x\ y} = AKi(U1_{x\ y+1} - U1_{x\ y-1} + U2_{x+1\ y} - U2_{x-1\ y})/8 \tag{76}$$

$$IU2_{x\ y} = AKi\{U1_{x+1\ y} - U1_{x-1\ y} + 3(U2_{x\ y+1} - U2_{x\ y-1})\}/8 \tag{77}$$

When there is a gradient in the y direction, this would correspond to y=3.5 and y=4.5 in Figure 3.

When x=10.5 (Figure 3), this is a gradient in the x-direction and the inhomogeneous parts take the form

$$IU1_{x\ y} = AKi\{3(U1_{x+1\ y} - U1_{x-1\ y}) + U2_{x\ y+1} - U2_{x\ y-1}\}/8 \tag{78}$$

$$IU2_{x\ y} = AKi(U1_{x\ y+1} - U1_{x\ y-1} + U2_{x+1\ y} - U2_{x-1\ y})/8 \tag{79}$$

Conditions / Models	Three Dimensional	Two Dimensional					
		Horizontal	Vertical	A	B	C	D
Area	Bowman, South Carolina, Area			Free Surface		Perturbations	
α_1 (Km/sec)	6.0	6.0	2.4	6.5	6.5	6.5	3.8
α_2 (Km/sec)	5.0	5.0	6.9		3.8	3.8	6.5
ρ_1 (gm/c.c.)	3.0	3.0	2.1	3.0	3.0	3.0	2.6
ρ_2 (gm/c.c.)	3.0	3.0	3.0		2.6	2.6	3.0
Initial Displacement	Linear Function	Cosine Curve	Cosine Curve	Cosine Curve	Cosine Curve	Cosine Curve	Cosine Curve
Top	Free Surface		Free Surface	Free Surface	Free Surface	Free Surface	Free Surface
Ends	Fixed	Fixed	Fixed	Fixed	Fixed	Fixed	Fixed
Bottom	Hydrostatic Restoring Pressure		Hydrostatic Restoring Pressure	Hydrostatic Restoring Pressure	Hydrostatic Restoring Pressure	Hydrostatic Restoring Pressure	Hydrostatic Restoring Pressure

Table 1. Boundary Conditions of 7 Models.

In equations (76-79) i=1 refers to points in the medium I and i=2 refers to points in the medium II.

Fixed Ends

Because of the implied symmetry of the cosine shaped hydrostatic driving stress, the two ends were constrained to movements in the $\pm$ U2 directions only. Then the following relation can be used to perform the computations at the edge of the grid,

$$U1_{1\ y}=0,\ U1_{2\ y}=-U1_{o\ y},\ U2_{2\ y}=U2_{o\ y} \tag{80}$$

$$U1_{21\ y}=0,\ U1_{20\ y}=-U1_{22\ y},\ U_{20\ y}=U2_{22\ y} \tag{81}$$

Using equations (80,81) and equations (55,56), one can directly write the equilibrium conditions at both ends in the form

$$U1_{1\ y} = U1_{21\ y} = 0 \tag{82}$$

$$U2_{1\ y} = \{3(U2_{1\ y+1} + U2_{1\ y-1}) + 2U2_{2\ y} + U1_{2\ y+1} - U1_{2\ y-1}\}/8 \tag{83}$$

$$U2_{21\ y} = \{3(U2_{21\ y+1} + U2_{21\ y-1}) + 2U2_{20\ y} - U1_{20\ y+1} + U1_{20\ y-1}\}/8 \tag{84}$$

Free Surface Top Computations

The free surface boundary conditions require that the stresses be zero,

$$\tau_{21} = \tau_{22} = 0 \tag{85}$$

or in differential equations form:

$$\frac{\partial U1}{\partial y} = -\frac{\partial U2}{\partial x}\Big|_{top} \tag{86}$$

$$\frac{\partial U2}{\partial y} = -\frac{1}{3}\frac{\partial U1}{\partial x}\Big|_{top} \tag{87}$$

Using the finite difference approximations, equations (86,87) become

$$U1_{x\ y+1} = U1_{x\ y-1} + U2_{x-1\ y} - U2_{x+1\ y} \tag{88}$$

$$U2_{x\ y+1} = (3U2_{x\ y-1} - U1_{x+1\ y} + U1_{x-1\ y})/3 \tag{89}$$

Substituting equations (80,81,88,89) into equations (55,56), the displacements equilibrium conditions for the top, are

$$U1_{x\ y} = \{8(U1_{x+1\ y} + U1_{x-1\ y}) + 6U1_{x\ y-1} + 3(U2_{x-1\ y} - U2_{x+1\ y})\}/22 \tag{90}$$

$$U2_{x\ y} = (6U2_{x\ y-1} + U1_{x-1\ y} - U1_{x+1\ y})/6 \tag{91}$$

In the reduction it was necessary to assume that

$$U1_{x-2\ y} - 2U1_{x\ y} + U1_{x+2\ y} \simeq 2(U1_{x-1\ y} - 2U1_{x\ y} + U1_{x+1\ y}) \tag{92}$$

$$U2_{x-2\ y} - 2U2_{x\ y} + U2_{x+2\ y} \simeq 2(U2_{x-1\ y} - 2U2_{x\ y} + U2_{x+1\ y}) \tag{93}$$

Hydrostatic-Pressure Bottom Computations

The boundary conditions of hydrostatic pressure, were developed by assuming that a purely normal stress was applied to the bottom such that,

$$\tau_{21} = 0 \tag{94}$$

$$\tau_{22} = f(x) \tag{95}$$

Where f(x) is an arbitrary function of position.

The function f(x) was assumed in this model to be a cosine function, such that the two sides would experience differential vertical forces. However, any reasonable function could have been used.

By introducing a restoring force proportional to the vertical displacement of the bottom $-\Delta\rho g U2_{x\ 1}$ the normal stress can be written as

$$\tau_{22} = f(x) = -\Delta\rho g\{U2_{x\ 1} - 0.05\cos[(x-1)\pi/20]\} \tag{96}$$

where $\Delta\rho$ is the density contrast, and

g is acceleration of gravity

From equation (96), the bottom boundary conditions are satisfied by taking,

$$\mu(3\frac{\partial U2}{\partial y} + \frac{\partial U1}{\partial x}) = \Delta\rho g\{-U2_{x\ 1} + 0.05\cos[(x-1)\pi/20]\} \tag{97}$$

In the deviation of the equations Poisson's relation ($\lambda=\mu$) was assumed, so that the shear wave velocity β can be computed from the P-wave velocities from $\beta=\alpha/\sqrt{3}$. In the model (Figure 3) the shear wave velocities were β_1=1.38 km/sec, and β_2=3.98 km/sec.

From equations (8,72,73), the elastic parameters are

$$\lambda_1 = \mu_1 = 4.032\cdot10^{10}\ \text{g/cm-sec}^2 = 4.032\cdot10^{4}\ \text{bars} \tag{98}$$

$$\lambda_2 = \mu_2 = 4.761\cdot10^{11}\ \text{g/cm-sec}^2 = 4.761\cdot10^{5}\ \text{bars} \tag{99}$$

Hence, one can express equation (97) in terms of displacement. Then

$$3(U2_{x\ y+1} - U2_{x\ y-1}) + U1_{x+1\ y} - U1_{x-1\ y}$$

$$= - D1 \cdot U2_{x\ 1} + E1 \cdot \cos[(x-1)\pi/20] \tag{100}$$

$$D1 = 2(\Delta x)(\Delta \rho) g/\mu_2 = 1.8525 \times 10^{-4} \tag{101}$$

$$E1 = 0.05 \cdot D1 = 9.2625 \times 10^{-6} \text{ cm} \tag{102}$$

$$D2 = D1/2 = 9.2625 \times 10^{-5} \tag{103}$$

$$E2 = E1/2 = 4.63125 \times 10^{-5} \text{ cm} \tag{104}$$

where $\Delta x = \Delta y = 0.5$ km

For the particular case of $y = 1$ (bottom), one finds on solving for $U2_{x\ o}$ from the stress conditions that

$$3U2_{x\ 0} = D1 \cdot U2_{x\ 1} + 3U2_{x\ y+1} + U1_{x+1\ 1} - U1_{x-1\ 1} - E1 \cdot \cos((x-1)\pi/20) \tag{105}$$

Solving equation (94) for $U1_{x\ y-1}$ one obtains

$$U1_{x\ y-1} = U1_{x\ y+1} + U2_{x+1\ y} - U2_{x-1\ y} \tag{106}$$

where $y = 1$

Substituting equations (80,81,90,91,105,106) into equations (55,56), the equilibrium conditions for displacements on the bottom, are

$$U1_{x\ y} = \{6U1_{x\ y+1} + 8(U1_{x+1\ y} + U1_{x-1\ y})(3-D2)(U2_{x+1\ y} - U2_{x-1\ y}) -$$

$$[E2 \cdot \cos((x-2)\pi/10) - \cos(x\pi/10)]\}/22 \tag{107}$$

$$U2_{x\ y} = [6U2_{x\ y+1} + U1_{x+1\ y} - U1_{x-1\ y} - E1 \cdot \cos(\frac{x-1}{20}\pi)]/(6 - D1) \qquad (108)$$

where $2 \leq x \leq 20$

$y = 1$

Four Corners Computations

Similarly by considering the symmetry of the boundary, one finds the following expressions for the displacements of the four corners.

$$U1_{1\ 1} = U1_{1\ 6} = U1_{21\ 1} = U1_{21\ 6} \qquad (109)$$

$$U2_{1\ 1} = (6U2_{1\ 2} + 2U1_{2\ 1} - E1)/(6-D1) \qquad (110)$$

$$U2_{1\ 6} = (6U2_{1\ 5} - 2U1_{2\ 6})/6 \qquad (111)$$

$$U2_{21\ 1} = (6U2_{21\ 2} - 2U1_{20\ 1} + E1)/(6-D1) \qquad (112)$$

$$U2_{21\ 6} = (6U2_{21\ 5} + 2U1_{20\ 6})/6 \qquad (113)$$

C Two-Dimensional Horizontal Model

The gravity contour lines suggest a two-dimensional horizontal structure as shown in Figure 4. The medium I is the high-velocity high-rigidity material. All of the properties of medium II are lower in magnitude than in medium I. The boundary conditions of this model are shown in Table 1. All the computations in this model are similar to those of the preceding vertical model. Therefore, the details of the equations will not be discussed in this section (refer to the computer program of Appendix I).

(IV) Initial Conditions and Methods of Solutions

Two-Dimensional Models

In the initial development of two-dimensional models the set of displacements were approximated by a set of cosine curves similar to the normal stress applied along the x-axis to the base and an amplitude along the y-axis of 0.1 km peak to peak for each curve (see Figure 5). The cosine function was used since it was the simplest function which would approximate the expected final solution.

By using the above values for the displacements as initial input data and equations (76-79,90,91,107-113) and the method of successive approximation (Timoshenko and Goodier, 1970), a computer program was developed which iteratively computes the displacement of each grid point (refer to program stress) until no farther change is observed.

Using the final displacements at each grid point and equations (59-69) the following can be evaluated; (1) principal stresses, (2) maximum shear stress, (3) strain energy per unit volume, (4) the angle between the axis of stresses and the coordinate axis.

Three-Dimensional Model

For the three-dimensional model, a linear function with maximum amplitudes of ± 50 meters along the y-axis (U2 direction) was used for the initial condition in the x direction. The method of successive approximation was used also in the three-dimensional model. Considering that too much computer time will be used in computation of the three-dimensional model, the displacements after each 100 or 200 iterations were saved for use as input data for next sequence of iterations.

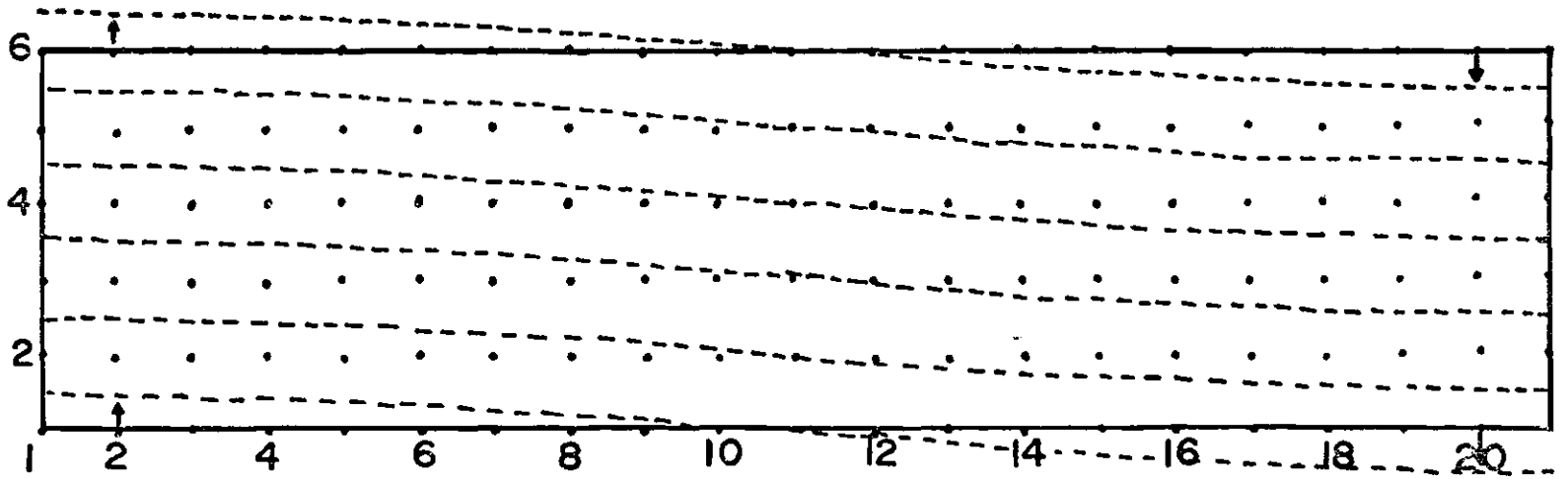

Figure 5. Initial Displacements at Each Grid Point (Cosine Curve with Amplitude of 50 Meters).

CHAPTER III

RESULTS AND DISCUSSION OF BOWMAN MODELS

Horizontal Model

Usually a material breaks on application of either of two different types of stresses, shearing stress or normal stress. The type of rupture that occurs depends on the machanical behavior of the material as well as the type of stress. Under tension the rupture usually occurs along a surface of maximum tensile stress. Under compression or shear the rupture usually occurs along planes of maximum shear stress. The horizontal shear model is designed to show the effects of imhomogeneities on applied shear or normal stress. Figure 6 shows the values and orientations for maximum shear stress at each grid point for the horizontal shear stress model resulting from application of a regional shear strain.

The stresses are symmetric about two axes because of the geometry of the central high-velocity and hence rigid structure. The stresses concentrated in the rigid material were from 1.5 to 2.0 times greater than in the immediately adjacent portions of the surrounding structure, and decreased outward in the surrounding low-velocity, low-rigidity material. In the surrounding material, the stresses were concentrated near the sharp corners. Figure 7 is a contour map of the magnitudes of the maximum shear stress for the horizontal shear stress model. The gradient along the long axis of the central rigid structure is low. If stress amplification is higher in a localized area such that the strength of the material is exceeded, then the material will rupture along the direction of the steepest

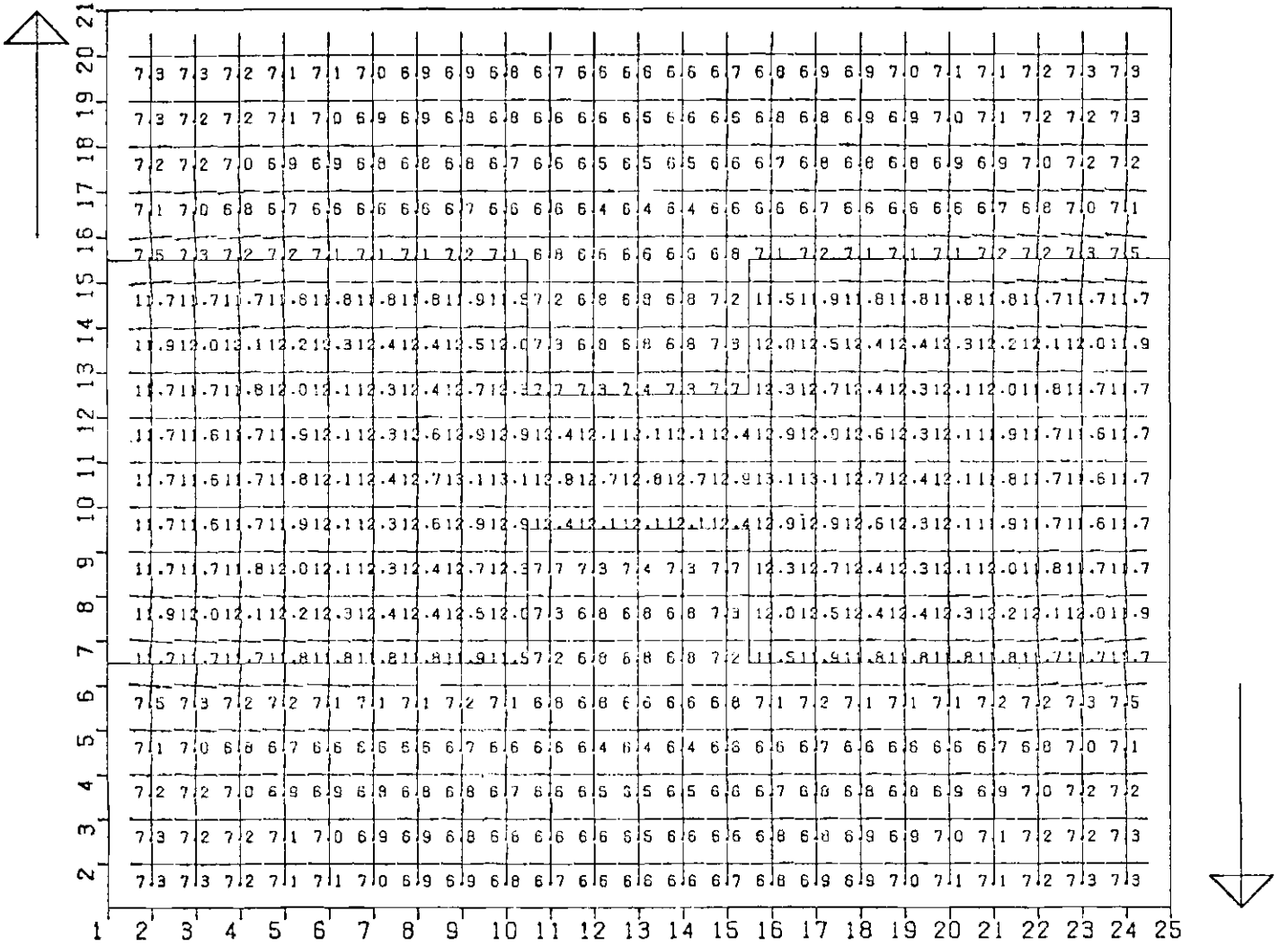

Figure 6. The Distribution of Maximum Shearing Stress of the Horizontal Model of Bowman Area.

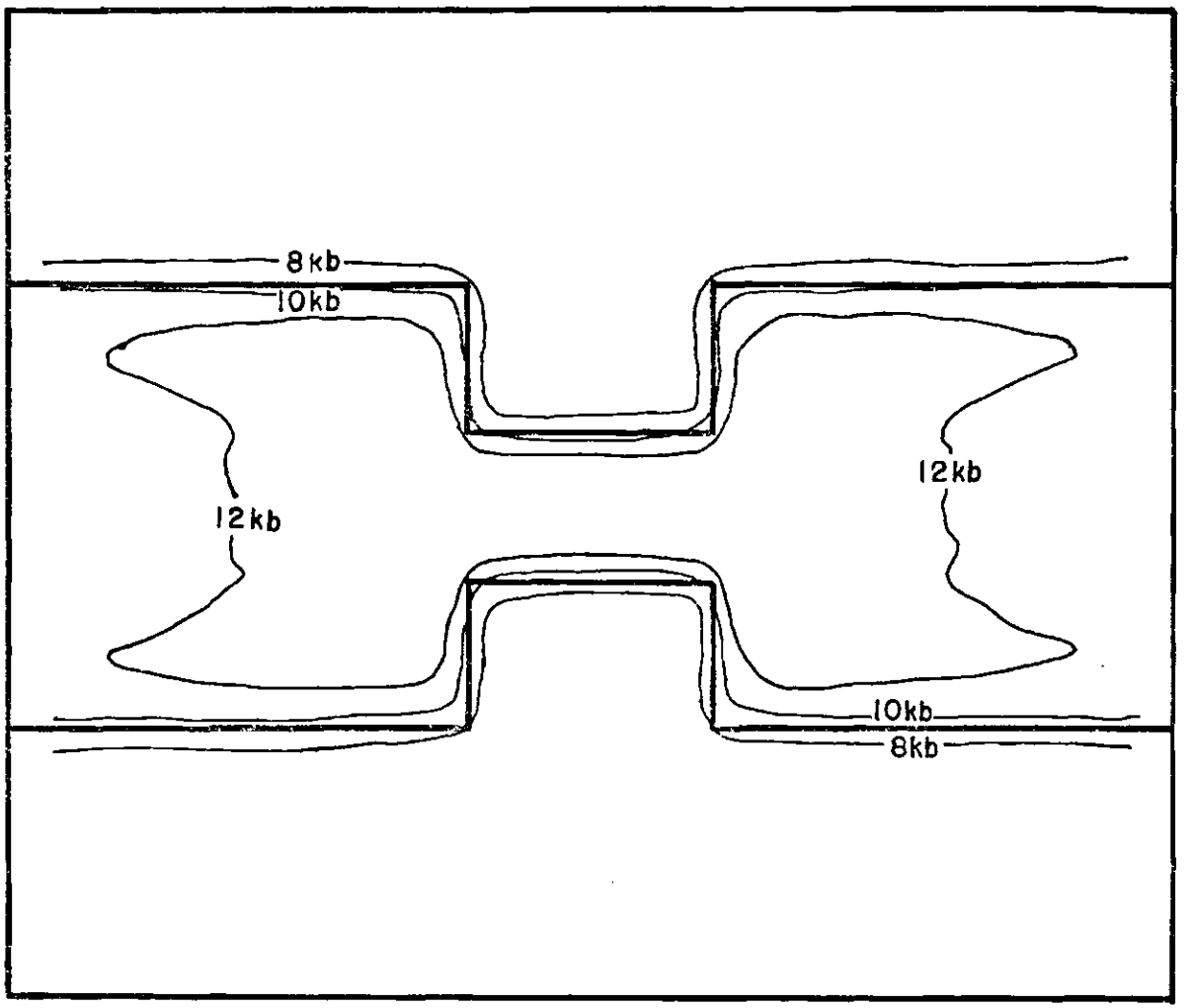

Figure 7. Contour Map of Maximum Shearing Stress of Horizontal Model of Bowman Area.

gradient, which in this case is normal to the axis of the of the structure.

Figure 8 shows the principal stress (normal stress) at each point for the horizontal shear stress model. The values are symmetric through the center. The stresses are concentrated in the thin central part of the high velocity structure. The orientation of the steepest gradient is toward the northwest.

Figure 9 shows the values of the strain energy per unit volume. The distribution of strain energy per unit volume is similar to the distribution of maximum shear stress (Figure 7). The strain energy per unit volume also shows four quadrant symmetry, high values inside the rigid body, and energy concentrated near the corners in the surrounding media. Combining the information in Figures (6,7,8,9), one can deduce the most likely plane for the occurrence of earthquakes, to be in the thin center portion along a direction from north to N 45° W. The microearthquake epicenters shown in Figure 1 are compatible with the horizontal stress model.

The above discussion of the model along with Figure 1 suggests that the epicenter locations correlate with the expected zone of stress con-concentrations.

Vertical Model

Figure 3 represents a vertical model with vertical uplift forces in the form of a cosine function applied to the bottom. The distribution of maximum shear stress (Figure 10) shows that the stresses are larger in the more rigid body, especially along the inhomogeneous boundary. The values in medium II are several times larger than in medium I. The high stresses concentrated at both ends of the structure are due to the

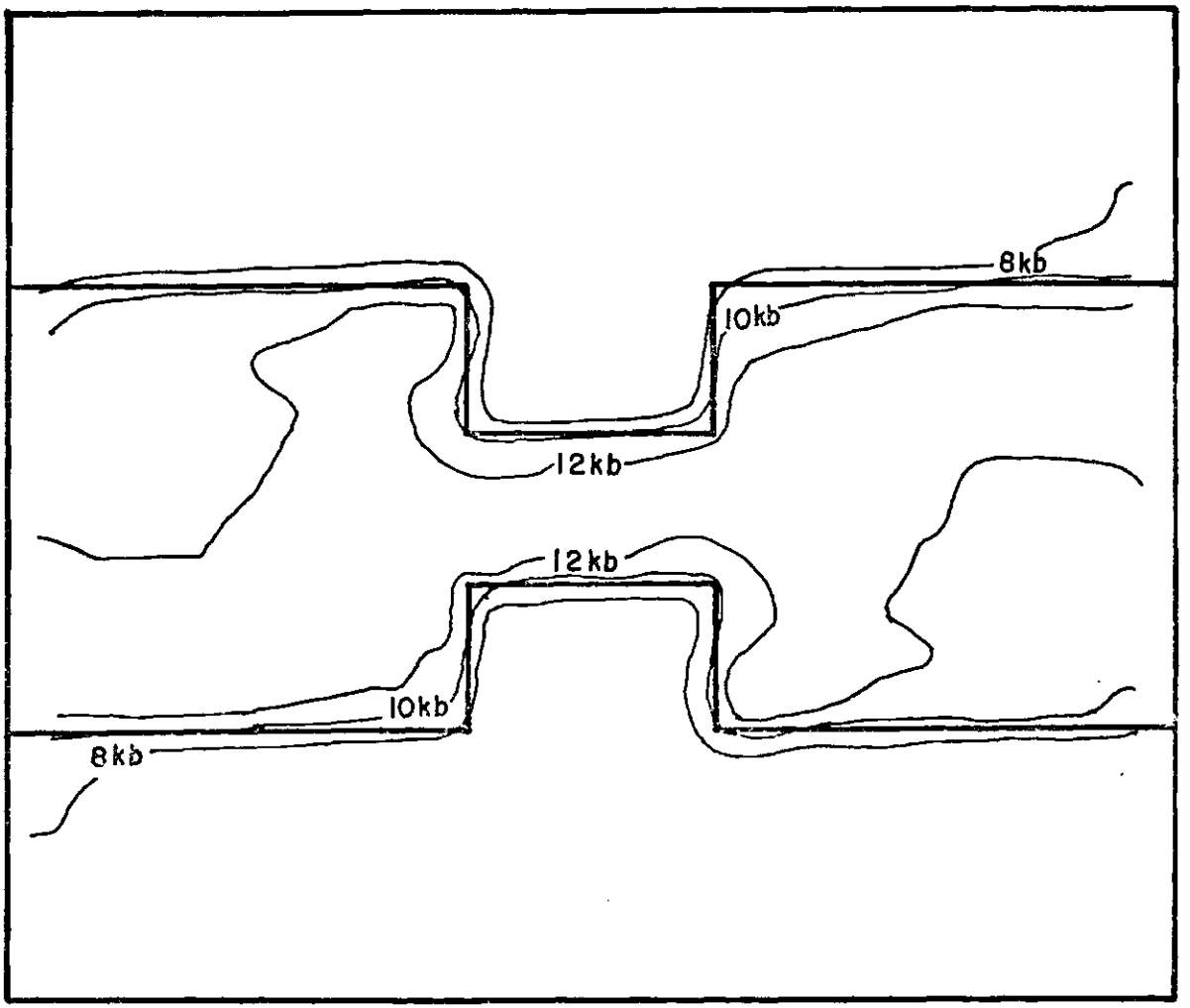

Figure 8. Contour Map of Principal Stress of Horizontal Model of Bowman Area.

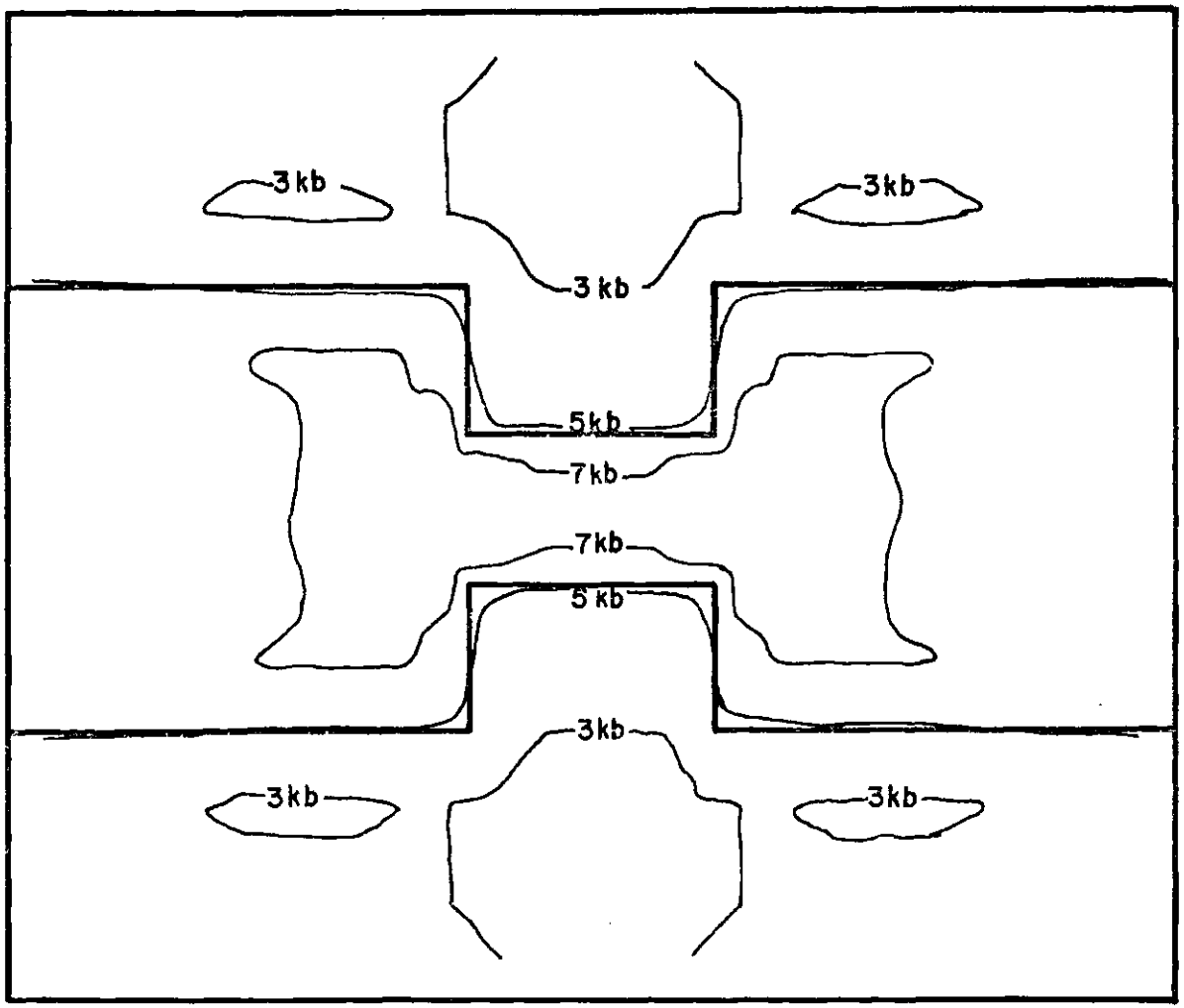

Figure 9. Contour Map of Strain Energy of the Horizontal Model of Bowman Area.

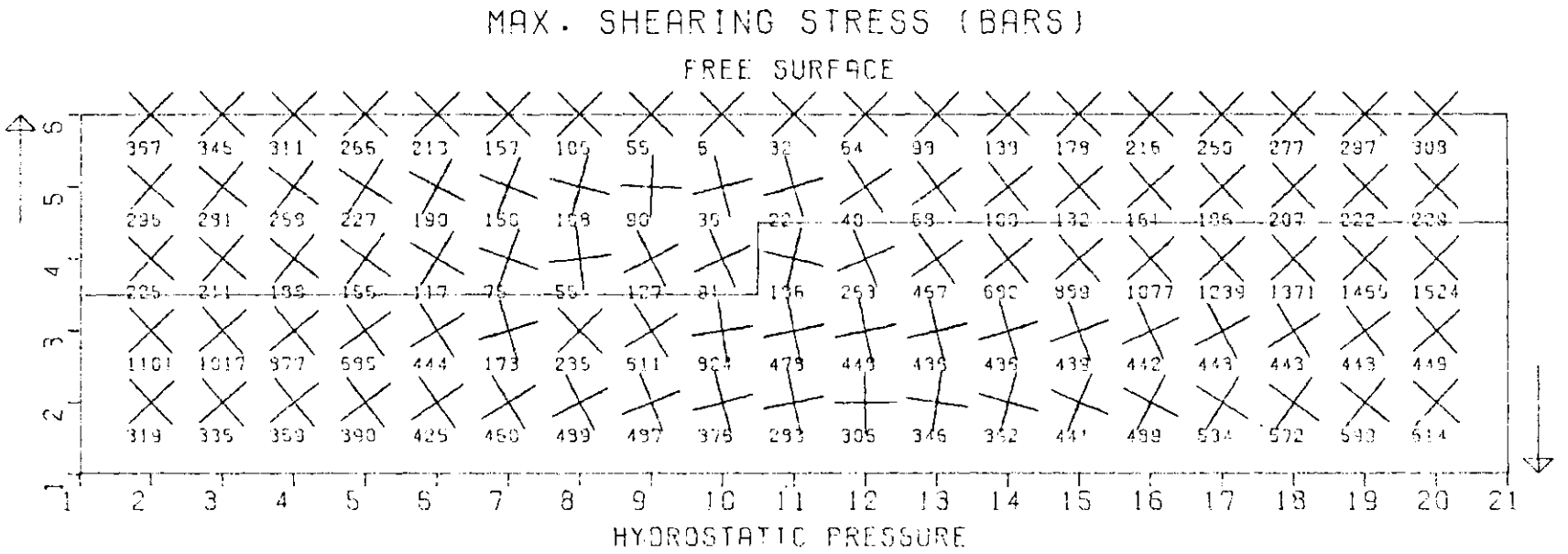

Figure 10. The Distribution of Maximum Shearing Stress of the Vertical Model of Bowman Area.

constraint of fixing the ends. Because of this the central portion provides a more meaningful result. Figure 11 is the enlarged central portion of the structure showing the planes of maximum shear stress. The orientations and magnitudes (Figure 11) of the maximum-shearing stresses at each grid point indicate that the sharp corner will foster the high stress contrast between the low velocity and high velocity material. The dotted lines represent the possible fault planes which are distorted by the boundary between the two materials. an important result shown in Figure 11 is the perturbation of the orientation of the fault planes which is due to the corner effect and change in thickness.

Figure 12 is a contour map of the maximum-shearing stress with a contour interval of 200 bars. The broad spacing of contours in medium I indicate less change in stress, whereas the sharp gradient or the dense grouping of the contour in medium II signifies the place of highest stress accumulation. Moreover, the corner area shows the highest stress with a maximum of 824 bars.

In medium I the stresses are significantly less than in medium II. This indicates that sedimentary overburden would be only minimally involved in earthquake mechanisms. (i. e., the stresses are decoupled by the contrast in μ).

Three-Dimensional Model

The stress distribution was also investigated in three-dimensions. The three-dimensional model and results are shown in Figure 13. The three diagrams in the lower left hand portion of Figure 13 show the maximum shear stress distribution for three plane sections (I=2,7,11). The stress

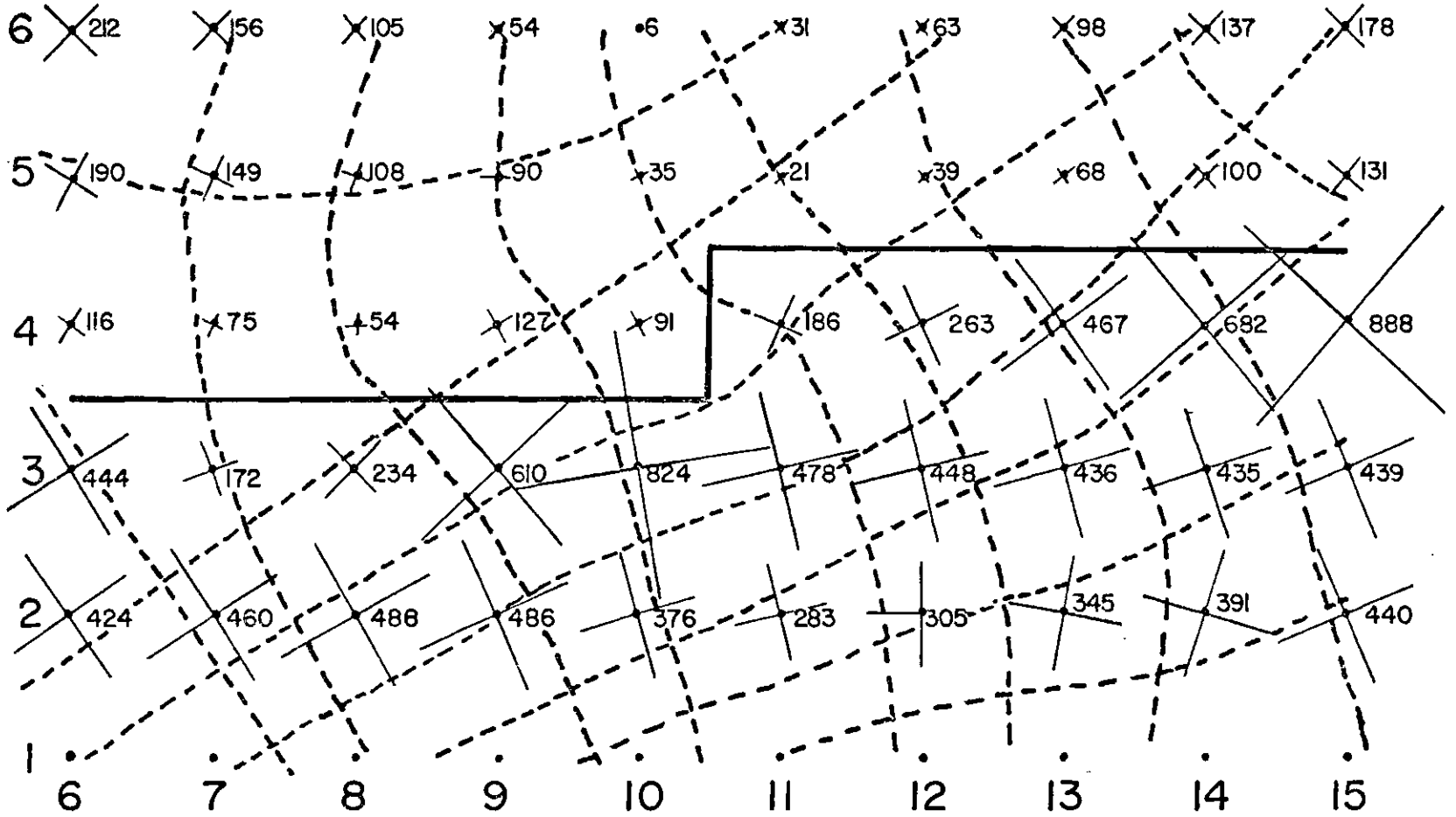

Figure 11. Fault Plane Orientation Estimate for Center Part of Vertical Model of Bowman Area.

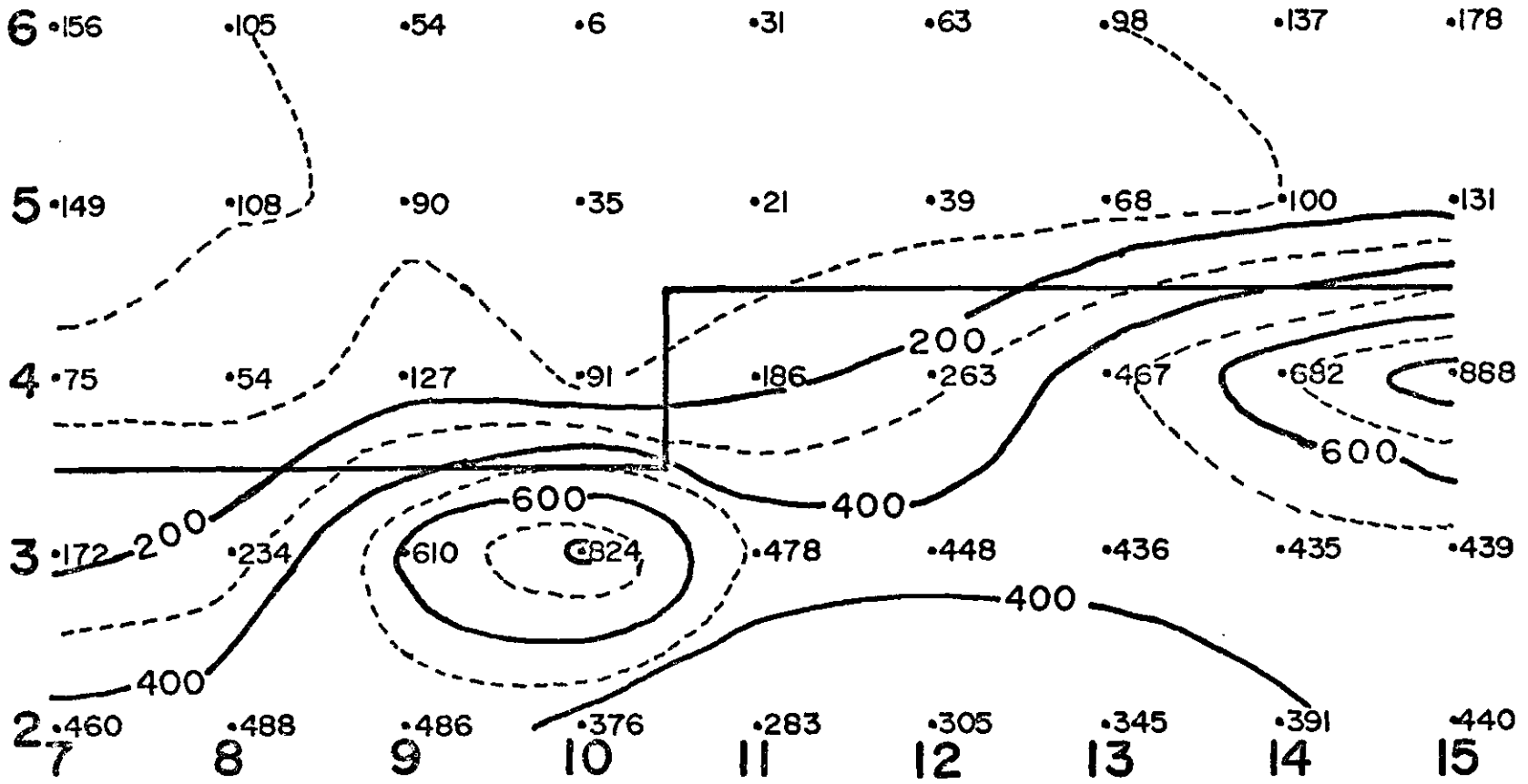

Figure 12. Contour Map of Center Part of the Vertical Model of Bowman Area.

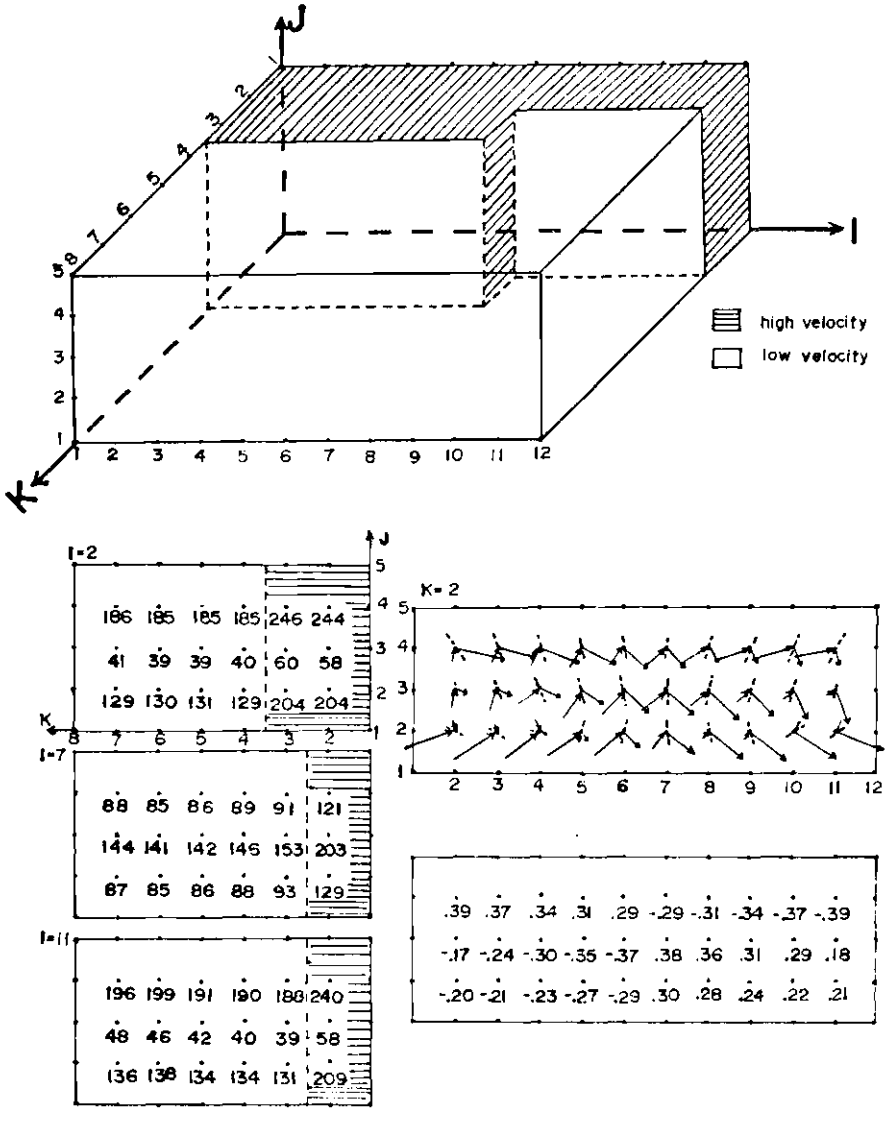

Figure 13. The Distribution of Stress of the Three-Dimensional Crustal Stress Model.

distributions are similar with a noted higher maximum shear stress accumulation in the high velocity material. In sections I=2 and II the upper and lower sampling lines indicate similar but higher values than the center line mainly because shear stress becomes a minimum at the geometric center of the couple. However, the section, I=7, is in direct contrast with the above two sections in that it shows a maximum shear stress in the center.

Another section (K=2) at right angles to the others is represented in the lower right hand portion of Figure 13. The upper diagram gives the directions of maximum shear stress (dotted lines), maximum principal stress (long solid line with arrow). The lower diagram gives the magnitudes of shear stress in kilo-bars for K=2. The direction and magnitude of stresses are affected by the near by geometry and thickness of the high-velocity material. The magnitudes of stress are higher where the material is thinner (I=8-11) as compared to the values where the materials is thicker (I=2-5) and the directions are perturbed near I=7.

CHAPTER IV

FREE SURFACE PERTURBATION

The free surface perturbation or change in stresses at the free surface will be discussed by considering the results or values of stress for three models shown in Figures 14(a,b,c,d). The boundary conditions are the same as for the previous vertical model.

Figures 15,16,17,18 show the values of maximum shearing stress corresponding to the models A,B,C,D shown in Figures 14A,14B,14C,14D.

Model A

The exposition shown in Figure 15 demonstrates the relation between a symmetric homogeneous-isotropic material and the resultant stress distribution. The center of the material exhibits a high concentration of stress. And because of fixing the ends high stress values occur at the four corners. Since the normal stress component is zero at the free surface the directions of maximum-shearing stresses at each grid point along the surface are 45° from the coordinate axis. The magnitude increases symmetrically outward (along x axis) from a central low stress value to the high values at the corners. If the corner effect is ignored the stress distribution possesses a center of symmetry which corresponds to the geometric center of the model. The magnitude decreases radially outward from the center value of 2 Kbar. This homogeneous model was computed to allow comparison with the other inhomogeneous models.

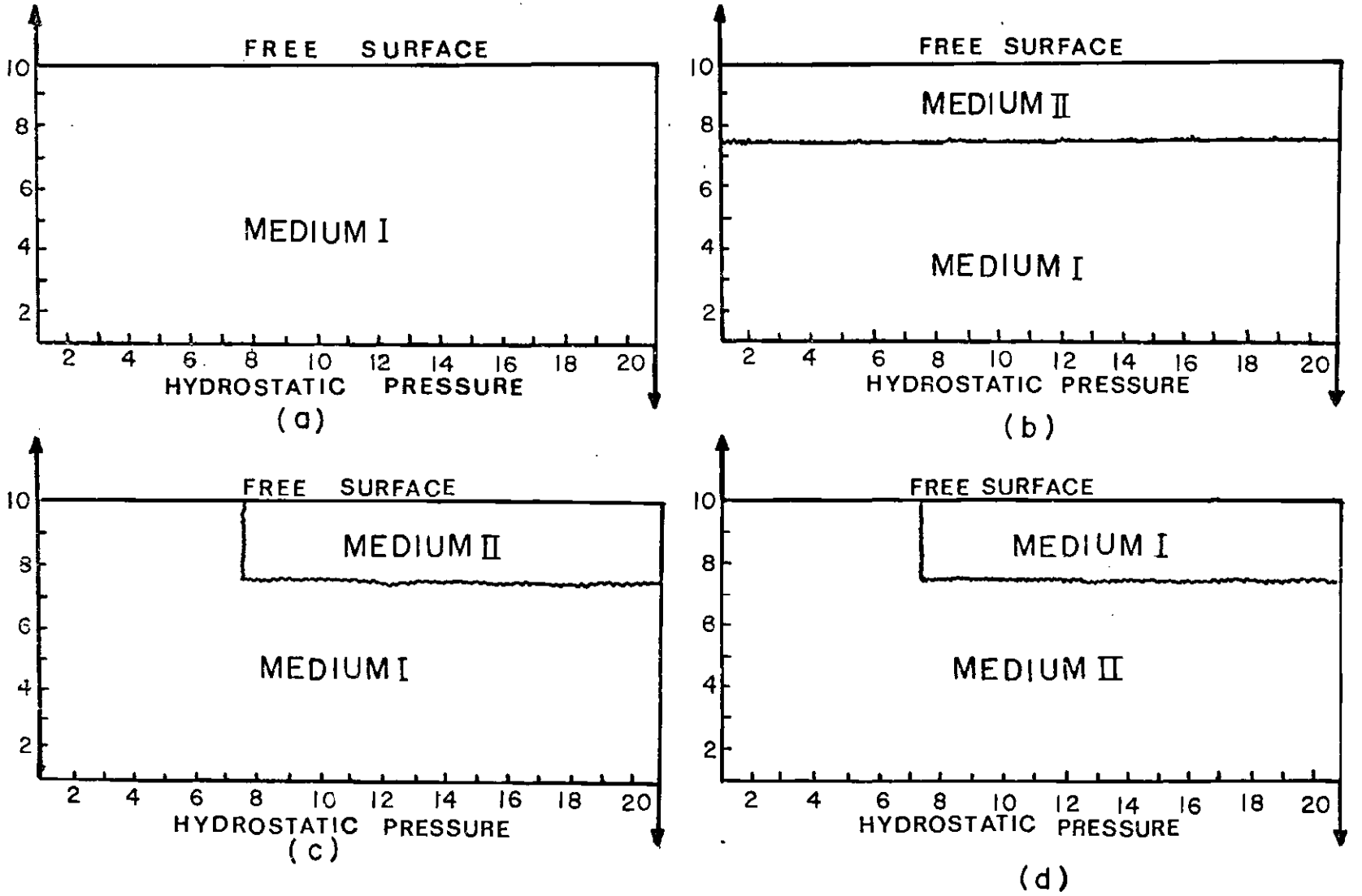

Figure 14. Mathematical Models (a) Model A (b) Model B (c) Model C (d) Model D.

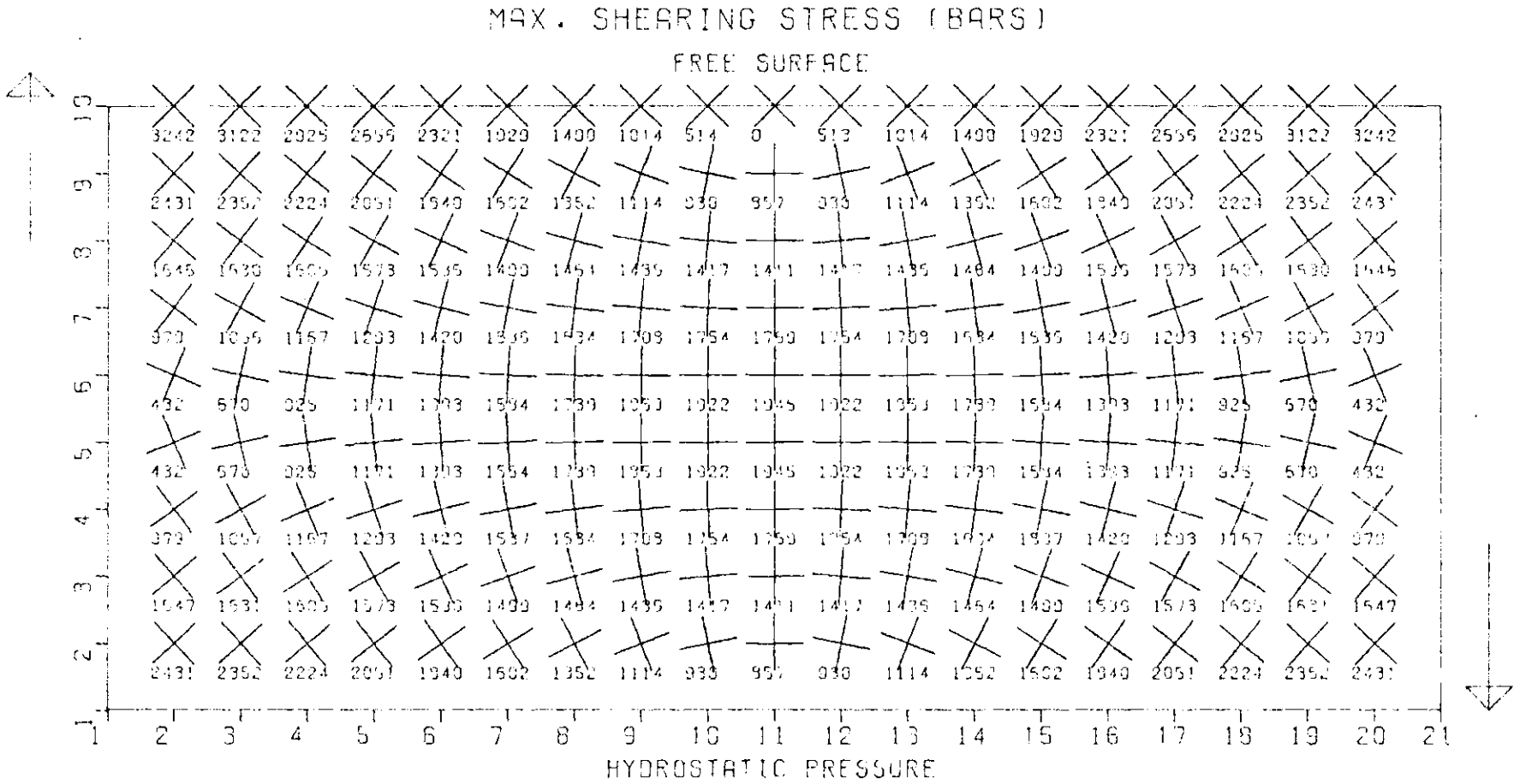

Figure 15. The Distribution of the Maximum Shearing Stress for Model A.

Model B

Figure 16 resolves the question as to what happens to the stress distribution when a rigid material is overlain by a less rigid material of lower velocity and density. The results indicate that both the magnitude and direction of stress change, the boundary between the two media behaves almost as a free surface. Figure 16 also shows a higher overall concentration of stress for the high rigidity material, especially at the boundary, as opposed to the overlying low rigidity material. The lower medium behaves similarly to the homogeneous model (Figure 15) in which the stress distribution possesses a geometric center of symmetry. Therefore, it appears that a thin overlying low-velocity low-density material only slightly affects the stress distribution and magnitude for a more rigid body.

Model C

As shown in Figure 17 the variation in stress in the right hand portion is about the same as in model B. In the vicinity of the sharp corner the stress is amplified in both materials. The upper left hand corner shows anomalously low stress values as compared to the variations in model A. This lowering of stress may be attributed to stress migration toward the corner area.

Model D

Model D in Figure 14 is identical to model C except medium I is reversed with medium II. The stress distribution for model D is shown in Figure 18. The stresses at the boundary and corner are about the same

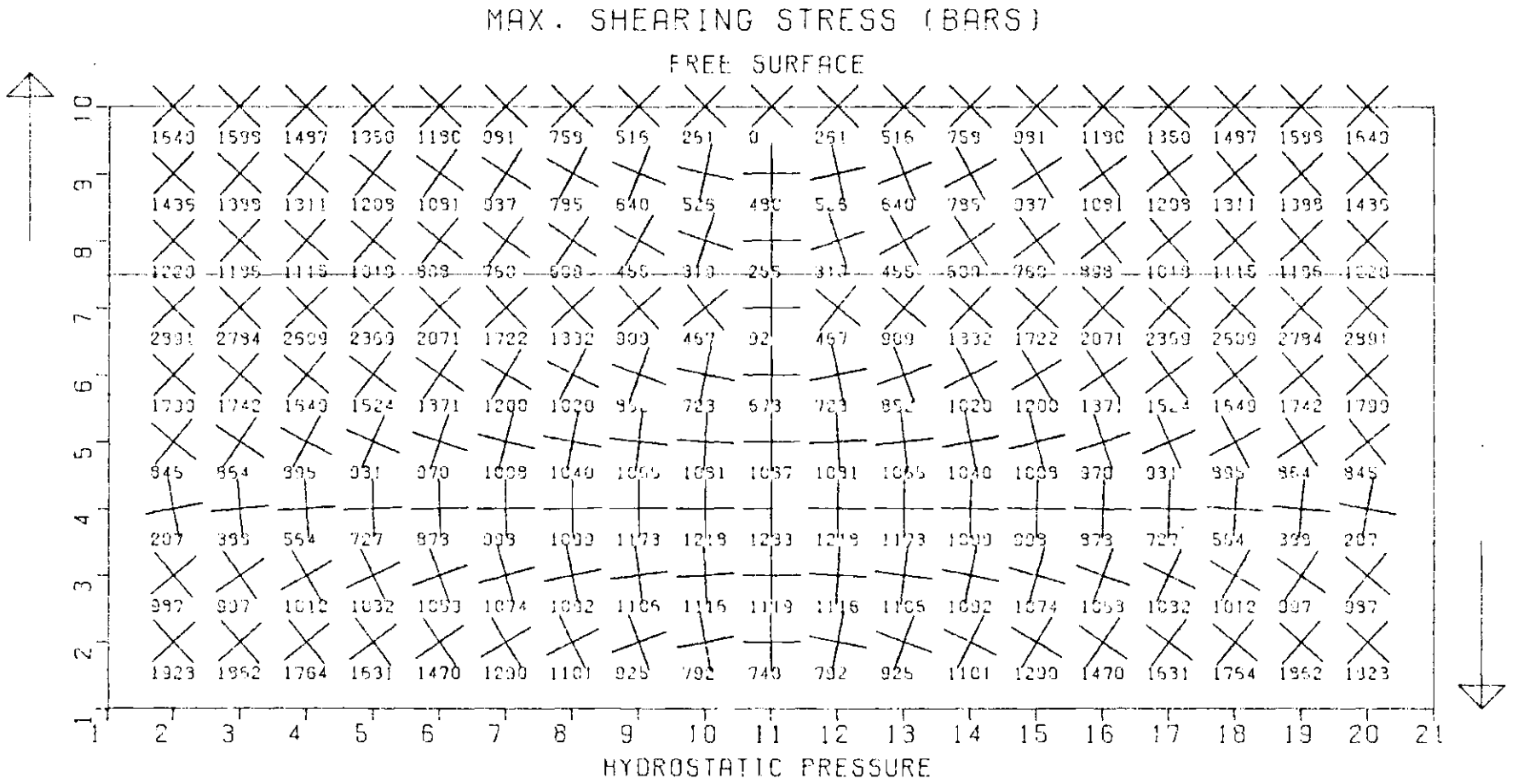

Figure 16. The Distribution of the Maximum Shearing Stress for Model B.

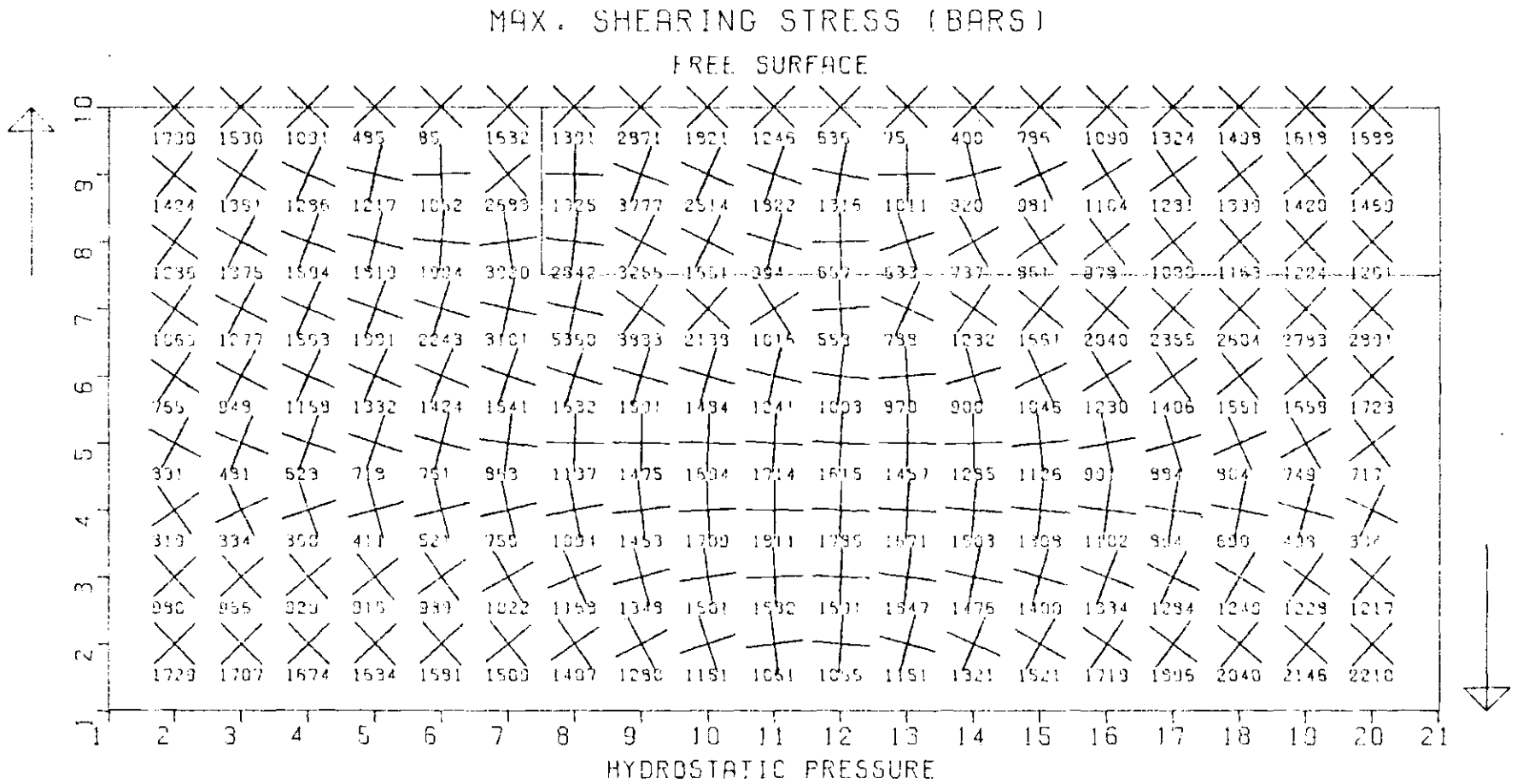

Figure 17. The Distribution of the Maximum Shearing Stress for Model C.

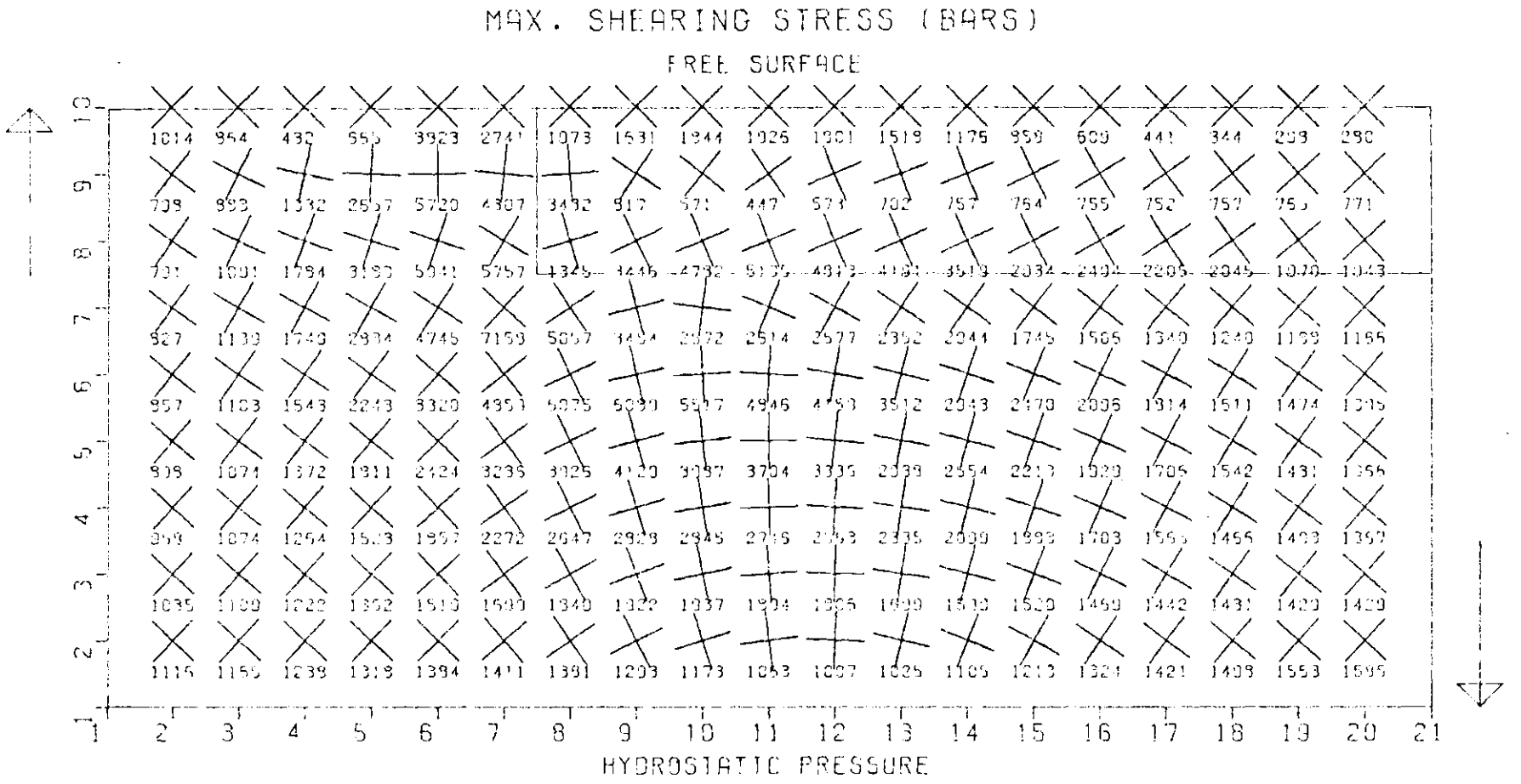

Figure 18. The Distribution of the Maximum Shearing Stress for Model D.

as in model C. But in this case the high-velocity high-density material does not contain the greater stress accumulation because of its small size, free surface boundary and floating state with respect to the lower medium. A rigid unit not completely coupled to applied stress or strain generates high stresses in the surrounding media rather than amplification within the rigid media.

CHAPTER V

CONCLUSIONS

The results of this study are summarized as follows:

(A) The stress field and resulting deformation are strongly dependent on the initial shape, internal structure, mechanical properties of the body, orientation of force vectors and the nature of applications (e.g. compressive, tensile, shear....).

(1) Higher stresses are concentrated in the more rigid portion of a model consisting of two different materials. In a model of two components, one having a low velocity and low density and the other having a high velocity and high density, a higher stress accumulation occurs in the high-velocity high-density material. Further the greater contrast in velocity and/or density between the two media the higher the stress accumulation..

(2) In general, the magnitude of stress is larger along the interface or boundary between the two layers.

(3) If the geometry of the model is such that a sharp corner exists the highest accumulation of stress occurs around this corner.

(B) In the case where a high-velocity high-density layer is overlain by a low-velocity low-density layer the top surface of the high-velocity layer acts as a free surface with the effect of the surface layer being minimum.

(C) Consider a small body of high velocity and high density immersed in a low-velocity low-density material or vice versa. The small body cannot concentrate a large amount of stress, but strongly influences stresses in surrounding material.

(D) Earthquakes in southeastern United States or in inhomogeneous media may occur along the surfaces which pass through the points having maximum magnitudes of shear stress.

CHAPTER VI

RECOMMENDATIONS

(1) Apply modeling technique to other seismically active area in the Southeast, such as: Jocasse Reservior Area (South Carolina), Charleston (South Carolina); and other intra-plate epicentral areas.

(2) By reducing the grid spacing to 0.1 KM or enlarging the size better resolution of the stress distribution may be obtained.

(3) Modify the shape or type of model in order to encompass a more varied structure.

(4) The viscosity of a rock depends on the shear stress. If the viscosity and or change in viscosity were known then the resulting stress distribution would be altered, perhaps to a more realistic representation.

APPENDIX I

PROGRAM LISTING

PRINTOUT OF " STRESS A " PROGRAM

```
      PROGRAM MAIN(INPUT,OUTPUT,PUNCH,TAPE5=INPUT,TAPE6=OUTPUT,TAPE7=
     CPUNCH,DEBUG=OUTPUT)
      DIMENSION U1(1050), U2(1050), T(6), IBUF(512)
       COMMON L1,L2,L3
       PI=3.14159
      NITER =200
      N = 2
      M = 1
      F1=-0.07638
      F2=-0.11
      G1=1.08E03
      G2=7.50E02
      WRITE(6,106)
  107 FORMAT(31HHORIZONTAL MODEL OF BOWMAN AREA)
      WRITE(6,107)
  106 FORMAT(//7HSTRESSA//)
C
C INITIAL INPUT
C
      DO 1 I=1,25
       AMP=0.05*(13-I)/10.
      DO 1 L=I,1050,25
      U2(L)=AMP
    1 CONTINUE
C
C ITERATE APPROXIMATION NITER TIMES
C
      DO 100 IT = 1,NITER
C
C HOMOGENEOUS COMPUTATIONS
C
      DO  10  I = 2,24
C
C COMPUTE INTERIOR POINTS
C
      DO 10 J=2,20
      CALL LOC(I,J,M)
      NEW=L2-(M-N)*525
```

PRINTOUT OF STRESSA (Continued)

```
      U1(NEW)=(3.*(U1(L2-1)+U1(L2+1))+U1(L1)+U1(L3)+0.5*(U2(L3+1)-
     C  U2(L3-1)-U2(L1+1)+U2(L1-1)))/8.
      U2(NEW)=(3.*(U2(L3)+U2(L1))+U2(L2-1)+U2(L2+1)+0.5*(U1(L3+1)-
     C  U1(L3-1)-U1(L1+1)+U1(L1-1)))/8.
   10 CONTINUE
C
C COMPUTE INHOMOGENIETY FACTOR
C IN HIGH-VEL MEDIA AK=F1
C IN LOW -VEL MEDIA AK=F2
C
      DO 200 I=2,15
       M1= 6+(I/11)*3
       M2= 7+(1/11)*3
       M3=15-(I/11)*3
       M4=16-(I/11)*3
      AK=F2
      DO 20 J=M1,M2
      CALL LOC(I,J,M)
      NEW=L2-(M-N)*525

      U1(NEW)=U1(NEW)+AK*(U1(L3)-U1(L1)+U2(L2+1)-U2(L2-1))/8.
      U2(NEW)=U2(NEW)+AK*(U1(L2+1)-U1(L2-1)+3.*(U2(L3)-U2(L1)))/8.
      AK=F1
   20 CONTINUE
      DO 200 J=M3,M4
      CALL LOC(I,J,M)
      NEW=L2-(M-N)*525
      U1(NEW)=U1(NEW)-AK*(U1(L3)-U1(L1)+U2(L2+1)-U2(L2-1))/8.
      U2(NEW)=U2(NEW)-AK*(U1(L2+1)-U1(L2-1)+3.*(U2(L3)-U2(L1)))/8.
      AK=F2
  200 CONTINUE
      DO 300 I=16,24
       M5= 6
       M6= 7
       M7=15
       M8=16
      AK=F2
      DO 30 J=M5,M6
      CALL LOC(I,J,M)
      NEW=L2-(M-N)*525
      U1(NEW)=U1(NEW)+AK*(U1(L3)-U1(L1)+U2(L2+1)-U2(L2-1))/8.
      U2(NEW)=U2(NEW)+AK*(U1(L2+1)-U1(L2-1)+3.*(U2(L3)-U2(L1)))/8.
      AK=F1
   30 CONTINUE
```

PRINTOUT OF STRESSA (Continued)

```
      DO 300 J=M7,M8
      CALL LOC(I,J,M)
      NEW=L2-(M-N)*525
      U1(NEW)=U1(NEW)-AK*(U1(L3)-U1(L1)+U2(L2+1)-U2(L2-1))/8.
      U2(NEW)=U2(NEW)-AK*(U1(L2+1)-U1(L2-1)+3.*(U2(L3)-U2(L1)))/8.
      AK=F2
  300 CONTINUE
       N1= 10
       N2=11
       N3=15
       N4=16
      DO 400 J=7,9
      AK=F1
      DO 40 I=N1,N2
      CALL LOC(I,J,M)
      NEW=L2-(M-N)*525
      U1(NEW)=U1(NEW)-AK*(3.*(U1(L2+1)-U1(L2-1))+U2(L3)-U2(L1))/8.
      U2(NEW)=U2(NEW)-AK*(U1(L3)-U1(L1)+U2(L2+1)-U2(L2-1))/8.
      AK=F2
   40 CONTINUE
      DO 400 I=N3,N4
      CALL LOC(I,J,M)
      NEW=L2-(M-N)*525
      U1(NEW)=U1(NEW)+AK*(3.*(U1(L2+1)-U1(L2-1))+U2(L3)-U2(L1))/8.
      U2(NEW)=U2(NEW)+AK*(U1(L3)-U1(L1)+U2(L2+1)-U2(L2-1))/8.
      AK=F1
  400 CONTINUE
      DO 500 J=13,15
      DO 50  I=N1,N2
      CALL LOC(I,J,M)
      NEW=L2-(M-N)*525
      U1(NEW)=U1(NEW)-AK*(3.*(U1(L2+1)-U1(L2-1))+U2(L3)-U2(L1))/8.
      U2(NEW)=U2(NEW)-AK*(U1(L3)-U1(L1)+U2(L2+1)-U2(L2-1))/8.
      AK=F2
   50 CONTINUE
      DO 500 I=N3,N4
      CALL LOC(I,J,M)
      NEW=L2-(M-N)*525
      U2(NEW)=U2(NEW)+AK*(U1(L3)-U1(L1)+U2(L2+1)-U2(L2-1))/8.
      U1(NEW)=U1(NEW)+AK*(3.*(U1(L2+1)-U1(L2-1))+U2(L3)-U2(L1))/8.
      AK=F1
  500 CONTINUE
      MSAV= M
      M = N
      N = MSAV
```

PRINTOUT OF STRESSA (Continued)

```
C
C  WRITE OUT RESULTS OF COMPUTATION
C
      IF(IT-(IT/200)*200) 100,51,100
   51 CONTINUE
      IH=1
      IF(IH.EQ.0) GO TO 301
      WRITE(6,105) IT
  105 FORMAT(/I10,37H      ITERATIONS      C DISPLACEMENTS 3/)
      I3=0
      DO 2 II=1,525,25
      I1=II
      I2=II+24
      I3=I3+1
      WRITE(6,101) I3
  101 FORMAT(1X,5H  J=  ,I2,13H,     I = 1,25)
      WRITE(6,102) (U1(I),I=I1,I2)
  102 FORMAT(1X,13F10.6)
      WRITE(6,102) (U2(I),I=I1,I2)
    2 CONTINUE
  301 CONTINUE
  100 CONTINUE
C
C COMPUTE THE PRINCIPAL STRESSES
C
      WRITE(6,104)
  104 FORMAT(//60H    I    J       PHI   MAX SHEAR  PRINCIPAL STRESSES  VOL
     CENERGY/)
      CALL PLOTS(IBUF,512,9,00)
      DO 110 IA=1,4
      IM=1
      IF(IM.EQ.0) GO TO 36
      CALL PLOT(5.0,3.0,-3)
      CALL RECT(0.0,0.0,6.0,7.2,0.0,2)
      CALL PLOT(0.00,1.65,+3)
      CALL PLOT(2.85,1.65,+2)
      CALL PLOT(2.85,2.55,+2)
      CALL PLOT(4.35,2.55,+2)
      CALL PLOT(4.35,1.65,+2)
      CALL PLOT(7.20,1.65,+2)
      CALL PLOT(7.20,4.35,+2)
      CALL PLOT(4.35,4.35,+2)
      CALL PLOT(4.35,3.45,+2)
      CALL PLOT(2.85,3.45,+2)
      CALL PLOT(2.85,4.35,+2)
```

PRINTOUT OF STRESSA (Continued)

```
      CALL PLOT(0.00,4.35,+2)
      CALL PLOT(0.00,1.65,+2)
      CALL SYMBOL(-0.9,4.5,1.5,19,0.0,-1)
      CALL SYMBOL(7.25,0.0,1.5,18,0.0,-1)
      DO 11 I=1,25
      X1=0.3*(I-1)
      X2=X1-0.1
      X3=1.0*I
      CALL SYMBOL(X1,-0.035,0.07,13,0.0,-1)
      CALL NUMBER(X2,-0.2,0.1,X3,0.0,-1)
   11 CONTINUE
      DO 12 J=2,21
      Y1=0.3*(J-1)
      Y2=Y1-0.1
      Y3=1.0*J
      CALL SYMBOL(-0.035,Y1,0.07,13,90.0,-1)
      CALL NUMBER(-0.1,Y2,0.1,Y3,90.0,-1)
   12 CONTINUE
   36 CONTINUE
      DO 21 I=2,24
      DO 21 J=2,20
      CALL LOC(I,J,M)
   41 T(1)=3.*(U1(L2+1)-U1(L2-1))+U2(L3)-U2(L1)
      T(2)=U1(L2+1)-U1(L2-1)+3.*(U2(L3)-U2(L1))
      T(3)=U2(L2+1)-U2(L2-1)+U1(L3)-U1(L1)
   42 IF(I.LT.11.AND.J.GT.6.AND.J.LT.16) GO TO 5
      IF(I.LT.16.AND.J.GT.9.AND.J.LT.13) GO TO 5
      IF(I.GT.15.AND.I.LT.25.AND.J.GT.6.AND.J.LT.16) GO TO 5
       AMU=G2
      GO TO 6
    5  AMU=G1
    6 CONTINUE
      DO 22 KK=1,3
      T(KK)=AMU*T(KK)
   22 CONTINUE
      A=(T(1)+T(2))/2.
      B=SQRT(((T(1)-T(2))/2)**2+T(3)*T(3))
      T(4)=A+B
      T(5)=A-B
      T(6)=B
      IF(T(1).NE.T(2)) GO TO 53
      PHI=45
      GO TO 52
   53 C=2.*T(3)/(T(1)-T(2))
      PHI1=0.5*ATAN(C)
      PHI=PHI1*180/PI
```

PRINTOUT OF STRESSA (Continued)

```
 52 V=(2*(T(1)*T(1)+T(2)*T(2))-T(1)*T(2)+3*T(3)*T(3))/(10*AMU)
    U=100*V
    IF(IM.EQ.0) GO TO 44
    WRITE(6,103) I,J,PHI,T(6),T(4),T(5),V
103 FORMAT(2I4,F10.2,4F10.4)
    GO TO 21
 44 X=0.3*(I-1)
    Y=0.3*(J-1)
    XX=X-0.1
    YY=Y-0.15
    IF(IA.EQ.1) CALL SPLOT(X,Y,XX,YY,T(6),PHI)
    IF(IA.EQ.2) CALL TPLOT(X,Y,XX,YY,T(6))
    IF(IA.EQ.3) CALL TPLOT(X,Y,XX,YY,T(4))
    IF(IA.EQ.4) CALL TPLOT(X,Y,XX,YY,U)
 21 CONTINUE
110 CONTINUE
    CALL PLOT(0,0,999)
    STOP
    END


    SUBROUTINE LOC(I,J,L)
    COMMON L1(3)
    M=0
    J1 = J + 1
    J3 = J - 1
    DO 10 JJ=J3,J1,1
    M = M + 1
    L1(M) = I+25*(JJ-1)+(L-1)*525
 10 CONTINUE
    RETURN
    END


    SUBROUTINE SPLOT(X,Y,XX,YY,T,PHI)
    P=-PHI
    CALL SYMBOL(X,Y,0.2,4,P,-1)
    CALL NUMBER(XX,YY,0.07,T,0.0,+1)
    RETURN
    END


    SUBROUTINE TPLOT(X,Y,XX,YY,T)
    CALL SYMBOL(X,Y,0.1,3,0.0,-1)
    CALL NUMBER(XX,YY,0.05,T,0.0,+1)
    RETURN
    END
```

PRINTOUT OF STRESS PROGRAM

```
      PROGRAM MAIN(INPUT,OUTPUT,PUNCH,TAPE5=INPUT,TAPE6=OUTPUT,TAPE7=
     CPUNCH)
      COMMON L1,L2,L3
      DIMENSION  U1(252),U2(252), T(6),IBUF(512)
      NITER =400
      PI = 3.14159
      N = 2
      M = 1
      D1= 1.8525E-4
      D2= 9.2625E-5
      E1= 9.2625E-6
      E2= 4.6312E-6
      F1=-0.2288279
      F2=-2.7020087
      G1= 4.0300E+4
      G2= 4.7610E+5
      WRITE(6,106)
  106 FORMAT(//6HSTRESS/)
C
C INITIAL INPUT
C
      DO 1 I=1,21
      AMP=COS((I-1)*PI/20)*0.05
      DO 1 L=I,252,21
      U2(L)=AMP
    1 CONTINUE
C
C ITERATE APPROXIMATION NITER TIMES
C
      DO 100 IT = 1,NITER
C
C HOMOGENEOUS COMPUTATIONS
C
      DO  90  I = 2,20
C
C COMPUTE INTERIOR POINTS
C
      DO 10 J=2,5
      CALL LOC(I,J,M)
      NEW=L2-(M-N)*126
      U1(NEW)=(3.*(U1(L2-1)+U1(L2+1))+U1(L1)+U1(L3)+0.5*(U2(L3+1)-
     C  U2(L3-1)-U2(L1+1)+U2(L1-1)))/8.
      U2(NEW)=(3.*(U2(L3)+U2(L1))+U2(L2-1)+U2(L2+1)+0.5*(U1(L3+1)-
     C  U1(L3-1)-U1(L1+1)+U1(L1-1)))/8.
   10 CONTINUE
```

PRINTOUT OF STRESS (Continued)

```
C
C COMPUTE THE TOP EDGE
C
      IA=1
      IF(IA.EQ.0) GO TO 90
      CALL LOC(I,6,M)
      NEW=L2-(M-N)*126
      U1(NEW)=(8.*(U1(L2-1)+U1(L2+1))+6.*U1(L1)+3.*(U2(L2-1)-U2(L2+1))
     C  22.
      U2(NEW)=(6.*U2(L1)+U1(L2-1)-U1(L2+1))/6.
C
C COMPUTE THE BOTTOM EDGE
C
      CALL LOC(I,1,M)
      NEW=L2-(M-N)*126
      U1(NEW)=(8.*(U1(L2+1)+U1(L2-1))+6.*U1(L3)+3.*(U2(L2+1)-U2(L2-1))
     C  -D2*(U2(L2+1)-U2(L2-1))-E2*(COS((I-2)*PI/20.)-COS(I*PI/20.)))/
      U2(NEW)=(6.*U2(L3)+U1(L2+1)-U1(L2-1)-E1*COS(PI*(I-1)/20.))/(6-D1
   90 CONTINUE
C
C COMPUTE TWO SIDES
C
      DO 20 J=2,5
      CALL LOC(1,J,M)
      NEW=L2-(M-N)*126
      U2(NEW)=(3.*(U2(L3)+U2(L1))+2.*U2(L2+1)+U1(L3+1)-U1(L1+1))/8.
      CALL LOC(21,J,M)
      NEW=L2-(M-N)*126
      CALL LOC(21,J,M)
      NEW=L2-(M-N)*126
      U2(NEW)=(3.*(U2(L3)+U2(L1))+2.*U2(L2-1)-U1(L3-1)+U1(L1-1))/8.
   20 CONTINUE
C
C COMPUTE FOUR CORNERS
C
      CALL LOC(1,1,M)
      NEW=L2-(M-N)*126
      U2(NEW)=(6.*U2(L3)+2.*U1(L2+1)-E1)/(6.-D1)
      CALL LOC(1,6,M)
      NEW=L2-(M-N)*126
      U2(NEW)=(6.*U2(L1)-2.*U1(L2+1))/6.
      CALL LOC(21,1,M)
      NEW=L2-(M-N)*126
      U2(NEW)=(6.*U2(L3)-2.*U1(L2-1)+E1)/(6.-D1)
      CALL LOC(21,6,M)
      NEW=L2-(M-N)*126
      U2(NEW)=(6.*U2(L1)+2.*U1(L2-1))/6.
```

PRINTOUT OF STRESS (Continued)

```
C
C  COMPUTE INHOMOGENIETY FACTOR
C  IN HIGH-VEL MEDIA AK=F1
C  IN LOW -VEL MEDIA AK=F2
C
C  INTERIOR POINTS (I DIRECTION )
C
      DO 70 I=2,20
      M1 =3+I/11
      M2 =4+I/11
      AK=F1
      DO 70 J=M1,M2
      CALL LOC(I,J,M)
      NEW=L2-(M-N)*126
      U1(NEW)=U1(NEW)+AK*(U1(L3)-U1(L1)+U2(L2+1)-U2(L2-1))/8.
      U2(NEW)=U2(NEW)+AK*(U1(L2+1)-U1(L2-1)+3.*(U2(L3)-U2(L1)))/8.
      AK=F2
   70 CONTINUE
C
C  COMPUTE BOTH SIDES
C
      AK=F1
      DO 60 J=3,4
      CALL LOC(1,J,M)
      NEW=L2-(M-N)*126
      U2(NEW)=U2(NEW)+AK*(2.*U1(L2+1)+3.*(U2(L3)-U2(L1)))/8.
      AK=F2
   60 CONTINUE
      AK=F1
      DO 40 J=4,5
      CALL LOC(21,J,M)
      NEW=L2-(M-N)*126
      U2(NEW)=U2(NEW)+AK*(-2.*U1(L2-1)+3.*(U2(L3)-U2(L1)))/8.
   40 CONTINUE
C
C  J DIRECTION
C
      AK=F2
      DO 50 I=10,11
      CALL LOC(I,4,M)
      NEW=L2-(M-N)*126
      U1(NEW)=U1(NEW)-AK*(3.*(U1(L2+1)-U1(L2-1))+U2(L3)-U2(L1))/8.
      U2(NEW)=U2(NEW)-AK*(U1(L3)-U1(L1)+U2(L2+1)-U2(L2-1))/8.
      AK=F1
   50 CONTINUE
```

PRINTOUT OF STRESS (Continued)

```
   37 MSAV= M
      M = N
      N = MSAV
C
C  WRITE OUT RESULTS OF COMPUTATION
C
      IF(IT-(IT/400)*400) 100,51,100
   51 CONTINUE
      IH=0
      IF(IH.EQ.0) GO TO 301
      WRITE(6,105) IT
  105 FORMAT(//I10,37H      ITERATIONS      [ DISPLACEMENTS ]/)
      DO 300 II=1,126,21
      I1=II
      I2=II+20
      WRITE(6,101) I1,I2
  101 FORMAT(1X,2I10)
      WRITE(6,102) (U1(I),I=I1,I2)
  102 FORMAT(1X,11F12.6)
      WRITE(6,102) (U2(I),I=I1,I2)
  300 CONTINUE
  301 CONTINUE
  100 CONTINUE
      IL=1
      IF(IL.EQ.0) GO TO 999
C COMPUTE THE PRINCIPAL STRESSES
C
      WRITE(6,104)
  104 FORMAT(//70H    I    J       PHI   MAX SHEAR  PRINCIPAL STRESSES  VO
     CENERGY    I      J/)
      IM=0
      IF(IM.EQ.0) GO TO 36
      CALL PLOTS(IBUF,512,9,00)
      CALL PLOT(3.0,3.0,-3)
      CALL RECT(0.0,0.0,2.0,8.0,0.0,2)
      CALL PLOT(0.0,1.0,+3)
      CALL PLOT(3.8,1.0,+2)
      CALL PLOT(3.8,1.4,+2)
      CALL PLOT(8.0,1.4,+2)
      CALL SYMBOL(3.4,2.2,0.1,12HFREE SURFACE,0.0,+12)
      CALL SYMBOL(3.0,-0.4,0.1,20HHYDROSTATIC PRESSURE,0.0,+20)
      CALL SYMBOL(-0.5,1.4,0.6,19,0.0,-1)
      CALL SYMBOL(8.0,0.0,0.6,18,0.0,-1)
      CALL SYMBOL(2.3,2.45,0.125,27HMAX. SHEARING STRESS (BARS),0.0,+2
```

PRINTOUT OF STRESS (Continued)

```
      DO 11 I=1,21
      X1=0.4*(I-1)
      X2=X1-0.1
      X3=1.0*I
      CALL SYMBOL(X1,-0.035,0.07,13,0.0,-1)
      CALL NUMBER(X2,-0.2,0.1,X3,0.0,-1)
   11 CONTINUE
      DO 12 J=1,6
      Y1=0.4*(J-1)
      Y2=Y1-0.1
      Y3=1.0*J
      CALL SYMBOL(-0.035,Y1,0.07,13,90.0,-1)
      CALL NUMBER(-0.1,Y2,0.1,Y3,90.0,-1)
   12 CONTINUE
   36 CONTINUE
      DO 21 I=2,20
      DO 21 J=2,6
      CALL LOC(I,J,M)
      IF(J.LT.6) GO TO 41
      T(1)=8*(U1(L2+1)-U1(L2-1))/3
      T(2)=0
      T(3)=0
      GO TO 42
   41 T(1)=3.*(U1(L2+1)-U1(L2-1))+U2(L3)-U2(L1)
      T(2)=U1(L2+1)-U1(L2-1)+3.*(U2(L3)-U2(L1))
      T(3)=U2(L2+1)-U2(L2-1)+U1(L3)-U1(L1)
      IF(I.LT.11.AND.J.LT.4) GO TO 5
      IF(I.GT.10.AND.J.LT.5) GO TO 5
   42 AMU=G1
      GO TO 6
    5 AMU=G2
    6 CONTINUE
      DO 22 KK=1,3
      T(KK)=AMU*T(KK)
   22 CONTINUE
      A=(T(1)+T(2))/2.
      B=SQRT(((T(1)-T(2))/2)**2+T(3)*T(3))
      T(4)=A+B
      T(5)=A-B
      T(6)=B
  212 IF(T(1).NE.T(2)) GO TO 53
      PHI=45

      GO TO 52
   53 C=2.*T(3)/(T(1)-T(2))
      PHI1=0.5*ATAN(C)
      PHI=PHI1*180/PI
```

PRINTOUT OF STRESS (Continued)

```
 52 V=(2*(T(1)*T(1)+T(2)*T(2))-T(1)*T(2)+5*T(3)*T(3))/(10*AMU)
    IF(IM.EQ.0) GO TO 44
    WRITE(6,103) I,J,PHI,T(6),T(4),T(5),V,I,J
103 FORMAT(2I4,F10.2,4F10.4,2I6)
 44 IF(IM.NE.0) CALL SPLOT(I,J,T(6),PHI)
 21 CONTINUE
    CALL PLOT(0,0,999)
999 STOP
    END



    SUBROUTINE LOC(I,J,L)
    COMMON L1(3)
    M=0
    J1 = J + 1
    J3 = J - 1
    DO 10 JJ=J3,J1,1
    M = M + 1
    L1(M) = I+21*(JJ-1)+(L-1)*126
 10 CONTINUE
    RETURN
    END



    SUBROUTINE SPLOT(I,J,T,PHI)
    X=0.4*(I-1)
    Y=0.4*(J-1)
    P=-PHI
    CALL SYMBOL(X,Y,0.25,4,P,-1)
    XX=X-0.13
    YY=Y-0.22
    CALL NUMBER(XX,YY,0.07,T,0.0,-1)
    RETURN
    END
```

APPENDIX II

RESULTS OF PROGRAM STRESSA

LISTING OF DISPLACEMENTS

STRESSA

HORIZONTAL MODEL OF BOWMAN AREA

200 ITERATIONS (DISPLACEMENTS)

J= 1, I = 1,25

U1	0.000000	0.000000	0.000000	0.000000	0.000000	0.000000	0.000000	0.000000	0.000000	0.000000	0.000000	0.000000	0.000000	0.000000	0.000000	0.000000	0.000000	0.000000	0.000000	0.000000	0.000000	0.000000	0.000000	0.000000	0.000000
	0.000000	0.000000	0.000000	0.000000	0.000000	0.000000	0.000000	0.000000	0.000000	0.000000	0.000000	0.000000	0.000000	0.000000	0.000000	0.000000	0.000000	0.000000	0.000000	0.000000	0.000000	0.000000	0.000000	0.000000	0.000000
U2	.000000	.000000	.000000	.000000	.000000	.000000	.000000	.000000	.000000	.000000	.000000	.000000	.000000	.000000	.000000	.000000	.000000	.000000	.000000	.000000	.000000	.000000	.000000	.000000	.000000
	.000000	.000000	.000000	.000000	.000000	.000000	.000000	.000000	.000000	.000000	.000000	.000000	.000000	.000000	.000000	.000000	.000000	.000000	.000000	.000000	.000000	.000000	.000000	.000000	.000000

J= 2, I = 1,25

	0.000000	.000132	.000184	.000236	.000306	.000333	.000379	.000427	.000479	.000532	.000584	.000636	.000688	.000740	.000792	.000844	.000896	.000948	.001000	.001052	.001104	.001156	.001208	.001260	.001312
	.000543	.000529	.000479	.000427	.000379	.000333	.000286	.000236	.000184	.000132	.000080	.000028	-.000024	-.000076	-.000128	-.000180	-.000232	-.000284	-.000336	-.000388	-.000440	-.000492	-.000544	-.000596	-.000648
	-.000756	-.000913	-.001402	-.001914	-.002430	-.002907	-.003366	-.003831	-.004289	-.004750	-.005211	-.005672	-.006133	-.006594	-.007055	-.007516	-.007977	-.008438	-.008899	-.009360	-.009821	-.010282	-.010743	-.011204	-.011665

J= 3, I = 1,25

	0.000000	.000152	.000289	.000418	.000536	.000641	.000732	.000812	.000880	.000936	.000980	.001012	.001032	.001040	.001036	.001020	.000992	.000952	.000900	.000836	.000760	.000672	.000572	.000460	.000336
	.000744	.000618	.000561	.000494	.000418	.000332	.000236	.000130	.000015	-.000110	-.000245	-.000390	-.000545	-.000710	-.000885	-.001070	-.001265	-.001470	-.001685	-.001910	-.002145	-.002390	-.002645	-.002910	-.003185
	-.003470	-.003765	-.004070	-.004385	-.004710	-.005045	-.005390	-.005745	-.006110	-.006485	-.006870	-.007265	-.007670	-.008085	-.008510	-.008945	-.009390	-.009845	-.010310	-.010785	-.011270	-.011765	-.012270	-.012785	-.013310

J= 4, I = 1,25

	0.000000	.000274	.000504	.000731	.000938	.001089	.001216	.001317	.001400	.001461	.001504	.001528	.001536	.001524	.001496	.001452	.001392	.001316	.001224	.001116	.000992	.000852	.000696	.000524	.000336
	.000132	-.000080	-.000280	-.000480	-.000680	-.000880	-.001080	-.001280	-.001480	-.001680	-.001880	-.002080	-.002280	-.002480	-.002680	-.002880	-.003080	-.003280	-.003480	-.003680	-.003880	-.004080	-.004280	-.004480	-.004680
	-.004880	-.005080	-.005280	-.005480	-.005680	-.005880	-.006080	-.006280	-.006480	-.006680	-.006880	-.007080	-.007280	-.007480	-.007680	-.007880	-.008080	-.008280	-.008480	-.008680	-.008880	-.009080	-.009280	-.009480	-.009680

J= 5, I = 1,25

	0.000000	.000424	.000828	.001174	.001453	.001647	.001732	.001716	.001626	.001490	.001336	.001174	.001022	.000896	.000812	.000784	.000816	.000912	.001072	.001296	.001584	.001936	.002352	.002832	.003376
	.003984	.004656	.005392	.006192	.007056	.007984	.008976	.010032	.011152	.012336	.013584	.014896	.016272	.017712	.019216	.020784	.022416	.024112	.025872	.027696	.029584	.031536	.033552	.035632	.037776
	.039984	.042256	.044592	.046992	.049456	.051984	.054576	.057232	.059952	.062736	.065584	.068496	.071472	.074512	.077616	.080784	.084016	.087312	.090672	.094096	.097584	.101136	.104752	.108432	.112176

J= 6, I = 1,25

	0.000000	.000765	.001364	.001822	.002147	.002419	.002592	.002691	.002716	.002677	.002577	.002424	.002227	.002000	.001752	.001492	.001232	.000984	.000760	.000572	.000432	.000352	.000344	.000420	.000592
	.000875	.001265	.001764	.002377	.003104	.003944	.004899	.005968	.007152	.008451	.009864	.011392	.013035	.014792	.016664	.018651	.020752	.022968	.025299	.027744	.030304	.032979	.035768	.038672	.041691
	.044825	.048074	.051438	.054917	.058512	.062221	.066046	.069986	.074041	.078211	.082496	.086896	.091411	.096041	.100786	.105646	.110621	.115711	.120916	.126236	.131671	.137221	.142886	.148666	.154561

J= 7, I = 1,25

	0.000000	.000925	.001729	.002379	.002879	.003242	.003481	.003612	.003652	.003617	.003524	.003388	.003224	.003048	.002876	.002722	.002600	.002524	.002508	.002564	.002704	.002940	.003284	.003748	.004344
	.005084	.005984	.007032	.008232	.009588	.011102	.012776	.014612	.016612	.018776	.021104	.023596	.026252	.029072	.032056	.035204	.038516	.041992	.045632	.049436	.053404	.057536	.061832	.066292	.070916

J= 8, I = 1,25

	0.000000	.000765	.001364	.001822	.002147	.002419	.002592	.002691	.002716	.002677	.002577	.002424	.002227	.002000	.001752	.001492	.001232	.000984	.000760	.000572	.000432	.000352	.000344	.000420	.000592
	.000875	.001265	.001764	.002377	.003104	.003944	.004899	.005968	.007152	.008451	.009864	.011392	.013035	.014792	.016664	.018651	.020752	.022968	.025299	.027744	.030304	.032979	.035768	.038672	.041691
	.044825	.048074	.051438	.054917	.058512	.062221	.066046	.069986	.074041	.078211	.082496	.086896	.091411	.096041	.100786	.105646	.110621	.115711	.120916	.126236	.131671	.137221	.142886	.148666	.154561

J= 9, I = 1,25

	0.000000	.000443	.000664	.000842	.000978	.001051	.001051	.001027	.000951	.000867	.000744	.000624	.000520	.000426	.000418	.000536	.000826	.001288	.001914	.002694	.003618	.004678	.005864	.007166	.008576
	.010094	.011709	.013412	.015194	.017047	.018963	.020933	.022950	.025006	.027093	.029203	.031328	.033460	.035591	.037713	.039818	.041898	.043946	.045954	.047914	.049818	.051659	.053429	.055120	.056724

J= 10, I = 1,25

	0.000000	.000206	.000314	.000418	.000520	.000626	.000750	.000909	.001106	.001362	.001693	.002104	.002591	.003145	.003753	.004396	.005052	.005695	.006294	.006815	.007225	.007487	.007564	.007419	.007014
	.006309	.005271	.003862	.002050	.000000	-.002426	-.005320	-.008826	-.013114	-.018365	-.024777	-.032564	-.041955	-.053198	-.066554	-.082307	-.100714	-.122025	-.146455	-.174236	-.205595	-.240775	-.280021	-.323592	-.371750

J= 11, I = 1,25

	0.000000	.000000	.000000	.000000	.000000	.000000	.000000	.000000	.000000	.000000	.000000	.000000	.000000	.000000	.000000	.000000	.000000	.000000	.000000	.000000	.000000	.000000	.000000	.000000	.000000
	.000000	.000000	.000000	.000000	.000000	.000000	.000000	.000000	.000000	.000000	.000000	.000000	.000000	.000000	.000000	.000000	.000000	.000000	.000000	.000000	.000000	.000000	.000000	.000000	.000000

LISTING OF DISPLACEMENTS (Continued)

.000000	.054590	.049353	.044231	.039148	.034117	.029046	.023930	.018721	.013634	.008809	.004373	-.000000
-.004373	-.008809	-.013634	-.018771	-.023930	-.029046	-.034117	-.039148	-.044231	-.049353	-.054590	-.060000	
J= 12.												
I = 1.25												
0.000000	-.000100	-.000206	-.000314	-.000418	-.000520	-.000626	-.000750	-.000909	-.001106	-.001362	-.001489	-.001537
-.001489	-.001362	-.001106	-.000909	-.000750	-.000626	-.000520	-.000418	-.000314	-.000206	-.000100	0.000000	
.000000	.004595	.049368	.044255	.039198	.034154	.029090	.023983	.018825	.013656	.008807	.004392	-.000000
-.004392	-.008807	-.013656	-.018825	-.023983	-.029090	-.034154	-.039198	-.044255	-.049368	-.054595	-.060000	
J= 13.												
I = 1.25												
0.000000	-.000218	-.000443	-.000684	-.000857	-.001051	-.001227	-.001413	-.001637	-.001914	-.002351	-.002394	-.002448
-.002394	-.002351	-.001914	-.001637	-.001413	-.001227	-.001051	-.000857	-.000684	-.000443	-.000218	0.000000	
.000000	.004613	.049418	.044328	.039285	.034253	.029204	.024117	.018963	.013671	.008754	.004433	-.000000
-.004433	-.008754	-.013671	-.018963	-.024117	-.029204	-.034253	-.039285	-.044328	-.049418	-.054613	-.060000	
J= 14.												
I = 1.25												
0.000000	-.000385	-.000765	-.001196	-.001595	-.001843	-.001829	-.001997	-.001148	-.002294	-.002415	-.002484	-.002504
-.002484	-.002415	-.002294	-.001148	-.001997	-.001829	-.001843	-.001595	-.001196	-.000765	-.000385	0.000000	
.000000	.004494	.049494	.044452	.039419	.034391	.029350	.024277	.019133	.013817	.008856	.004494	-.000000
-.004494	-.008856	-.013817	-.019133	-.024277	-.029350	-.034391	-.039419	-.044452	-.049494	-.054658	-.060000	
J= 15.												
I = 1.25												
0.000000	-.000701	-.001375	-.002079	-.002342	-.002531	-.002342	-.002679	-.002704	-.003699	-.003611	-.002796	-.002585
-.002796	-.003611	-.003699	-.002704	-.002679	-.002342	-.002531	-.002342	-.002079	-.001375	-.000701	0.000000	
.000000	.004575	.049407	.044407	.039407	.034407	.029407	.024418	.019283	.014006	.009016	.004520	-.000000
-.004520	-.009016	-.014006	-.019283	-.024418	-.029495	-.034546	-.039586	-.044627	-.049682	-.054775	-.060000	
J= 16.												
I = 1.25												
0.000000	-.000755	-.001364	-.001822	-.002167	-.002419	-.002592	-.002891	-.002716	-.003877	-.003549	-.002495	-.002475
-.002495	-.003549	-.003877	-.002716	-.002891	-.002592	-.002419	-.002167	-.001822	-.001364	-.000755	0.000000	
.000000	.004575	.049407	.044407	.039407	.034407	.029407	.024407	.019407	.014259	.009285	.004635	-.000000
-.004635	-.009285	-.014259	-.019407	-.024407	-.029519	-.034690	-.039753	-.044817	-.049837	-.054957	-.060000	
J= 17.												
I = 1.25												
0.000000	-.000624	-.000939	-.001174	-.001453	-.001667	-.001822	-.001926	-.001990	-.002035	-.002074	-.002104	-.002111
-.002104	-.002074	-.002035	-.001990	-.001926	-.001822	-.001667	-.001453	-.001174	-.000938	-.000624	0.000000	
.000000	.004715	.049424	.044466	.039466	.034467	.029723	.024738	.019622	.014474	.009474	.004715	-.000000
-.004715	-.009474	-.014429	-.019622	-.024738	-.029723	-.034807	-.039866	-.044966	-.050043	-.055089	-.060000	
J= 18.												
I = 1.25												
0.000000	-.000554	-.000731	-.000920	-.001019	-.001216	-.001117	-.001400	-.001481	-.001551	-.001618	-.001634	
-.001618	-.001551	-.001481	-.001400	-.001216	-.001019	-.000920	-.000731	-.000504	-.000256	0.000000		
.000000	.052122	.050113	.045053	.039978	.034901	.029822	.024740	.019650	.014609	.009849	.004804	-.000000
-.004804	-.009849	-.014609	-.019650	-.024740	-.029822	-.034901	-.039978	-.045053	-.050113	-.055122	-.060000	
J= 19.												
I = 1.25												
0.000000	-.000152	-.000299	-.000418	-.000536	-.000641	-.000742	-.000812	-.000889	-.000960	-.001044	-.001098	-.001117
-.001098	-.001044	-.000960	-.000889	-.000812	-.000742	-.000641	-.000536	-.000418	-.000299	-.000152	0.000000	
.000000	.055110	.050118	.045080	.039966	.034907	.029907	.024848	.019797	.014770	.009884	.004884	-.000000
-.004884	-.009884	-.014770	-.019797	-.024848	-.029907	-.034966	-.040025	-.045080	-.050118	-.055110	-.060000	
J= 20.												
I = 1.25												
0.000000	-.000574	-.000832	-.000984	-.000916	-.000343	-.000429	-.000343	-.000429	-.000427	-.000479	-.000543	-.000574
-.000543	-.000479	-.000427	-.000343	-.000343	-.000343	-.000343	-.000238	-.000184	-.000172	-.000076	0.000000	
.000000	.055059	.050077	.045059	.040031	.035000	.029968	.024930	.019914	.014902	.009913	.004950	-.000000
-.004950	-.009913	-.014902	-.019914	-.024930	-.029968	-.035000	-.040031	-.045059	-.050077	-.055069	-.060000	
J= 21.												
I = 1.25												
0.000000	0.000000	0.000000	0.000000	0.000000	0.000000	0.000000	0.000000	0.000000	0.000000	0.000000	0.000000	0.000000
0.000000	0.000000	0.000000	0.000000	0.000000	0.000000	0.000000	0.000000	0.000000	0.000000	0.000000	0.000000	
.000000	.055000	.050000	.045000	.040000	.035000	.030000	.025000	.020000	.015000	.010000	.005000	0.000000
-.005000	-.010000	-.015000	-.020000	-.025000	-.030000	-.035000	-.040000	-.045000	-.050000	-.055000	-.060000	

LISTING OF PARAMETERS

I	J	PHI	MAX SHEAR	PRINCIPAL STRESSES		VOL ENERGY
2	2	-44.94	7.3283	7.6904	-6.9662	.0359
2	3	-44.30	7.2785	7.7931	-6.7639	.0354
2	4	-43.44	7.2225	7.9477	-6.4973	.0350
2	5	-42.00	7.1252	8.1195	-6.1308	.0342
2	6	-40.16	7.4837	9.0590	-5.9084	.0383
2	7	-40.81	11.6781	13.7867	-9.5696	.0644
2	8	-42.58	11.8874	13.1891	-10.5857	.0659
2	9	-43.66	11.7491	12.5696	-10.9286	.0641
2	10	-44.40	11.7199	12.1157	-11.3242	.0636
2	11	-45.00	11.7154	11.7154	-11.7154	.0635
2	12	44.40	11.7199	11.3242	-12.1157	.0636
2	13	43.66	11.7491	10.9286	-12.5696	.0641
2	14	42.58	11.8874	10.5857	-13.1891	.0659
2	15	40.81	11.6781	9.5696	-13.7867	.0644
2	16	40.16	7.4837	5.9084	-9.0590	.0383
2	17	42.00	7.1252	6.1308	-8.1195	.0342
2	18	43.44	7.2225	6.4973	-7.9477	.0350
2	19	44.30	7.2785	6.7639	-7.7931	.0354
2	20	44.94	7.3283	6.9662	-7.6904	.0359
3	2	44.97	7.2904	7.6298	-6.9511	.0355
3	3	-44.32	7.2454	7.6985	-6.7923	.0351
3	4	-43.35	7.1605	7.7618	-6.5591	.0343
3	5	-41.99	6.9854	7.7718	-6.1991	.0328
3	6	-40.84	7.3470	8.3900	-6.3041	.0364
3	7	-41.29	11.7045	13.1229	-10.2862	.0640
3	8	-42.45	11.9684	12.9570	-10.9798	.0666
3	9	-43.43	11.7291	12.3750	-11.0831	.0638
3	10	-44.26	11.6495	11.9699	-11.3292	.0629
3	11	-45.00	11.6323	11.6323	-11.6323	.0626
3	12	44.26	11.6495	11.3292	-11.9699	.0629
3	13	43.43	11.7291	11.0831	-12.3750	.0638
3	14	42.45	11.9684	10.9798	-12.9570	.0666
3	15	41.29	11.7045	10.2862	-13.1229	.0640
3	16	40.84	7.3470	6.3041	-8.3900	.0364
3	17	41.99	6.9854	6.1991	-7.7718	.0328
3	18	43.35	7.1605	6.5591	-7.7618	.0343
3	19	44.32	7.2454	6.7923	-7.6985	.0351
3	20	-44.97	7.2904	6.9511	-7.6298	.0355
4	2	-44.93	7.2208	7.4968	-6.9447	.0348
4	3	-44.24	7.1615	7.5226	-6.8004	.0342
4	4	-43.36	7.0457	7.5114	-6.5799	.0332
4	5	-42.29	6.8305	7.4150	-6.2461	.0312
4	6	-41.60	7.3351	7.9299	-6.5402	.0351

LISTING OF PARAMETERS (Continued)

4	7	-41.92	11.7434	12.6901	-10.7966	.0641
4	8	-42.62	12.0959	12.8100	-11.3818	.0679
4	9	-43.37	11.8187	12.3074	-11.3301	.0647
4	10	-44.18	11.7057	11.9548	-11.4565	.0635
4	11	-45.00	11.6776	11.6776	-11.6776	.0631
4	12	44.18	11.7057	11.4565	-11.9548	.0635
4	13	43.37	11.8187	11.3301	-12.3074	.0647
4	14	42.62	12.0959	11.3818	-12.8100	.0679
4	15	41.92	11.7434	10.7966	-12.6901	.0641
4	16	41.60	7.2351	6.5402	-7.9299	.0351
4	17	42.29	6.8305	6.2461	-7.4150	.0312
4	18	43.36	7.0457	6.5799	-7.5114	.0332
4	19	44.24	7.1615	6.8004	-7.5226	.0342
4	20	44.93	7.2208	6.9447	-7.4968	.0348
5	2	-44.77	7.1424	7.3327	-6.9520	.0340
5	3	-44.16	7.0692	7.3244	-6.8140	.0333
5	4	-43.46	6.9362	7.2640	-6.6084	.0321
5	5	-42.70	6.7122	7.1139	-6.3106	.0301
5	6	-42.30	7.1580	7.6041	-6.7118	.0342
5	7	-42.51	11.7653	12.3691	-11.1614	.0642
5	8	-42.90	12.2079	12.6949	-11.7209	.0691
5	9	-43.42	11.9547	12.3134	-11.5960	.0662
5	10	-44.15	11.8509	12.0428	-11.6590	.0650
5	11	-45.00	11.8262	11.8262	-11.8262	.0647
5	12	44.15	11.8509	11.6590	-12.0428	.0650
5	13	43.42	11.9547	11.5960	-12.3134	.0662
5	14	42.90	12.2079	11.7209	-12.6949	.0691
5	15	42.51	11.7653	11.1614	-12.3691	.0642
5	16	42.30	7.1580	6.7118	-7.6041	.0342
5	17	42.70	6.7122	6.3106	-7.1139	.0301
5	18	43.46	6.9362	6.6084	-7.2640	.0321
5	19	44.16	7.0692	6.8140	-7.3244	.0333
5	20	44.77	7.1424	6.9520	-7.3327	.0340
6	2	-44.60	7.0671	7.1624	-6.9718	.0333
6	3	-44.10	6.9902	7.1355	-6.8449	.0326
6	4	-43.59	6.8559	7.0496	-6.6622	.0314
6	5	-43.12	6.6391	6.8757	-6.4025	.0294
6	6	-42.92	7.1130	7.3607	-6.8652	.0338
6	7	-43.03	11.7754	12.1077	-11.4431	.0642
6	8	-43.17	12.2941	12.5977	-11.9904	.0700
6	9	-43.47	12.1068	12.3714	-11.8423	.0679
6	10	-44.12	12.0579	12.2143	-11.9015	.0673
6	11	45.00	12.0547	12.0547	-12.0547	.0673
6	12	44.12	12.0579	11.9015	-12.2143	.0673
6	13	43.47	12.1068	11.8423	-12.3714	.0679
6	14	43.17	12.2941	11.9904	-12.5977	.0700

LISTING OF PARAMETERS (Continued)

6	15	43.03	11.7754	11.4431	-12.1077	.0642
6	16	42.92	7.1130	6.8652	-7.3607	.0338
6	17	43.12	6.6391	6.4025	-6.8757	.0294
6	18	43.59	6.8559	6.6622	-7.0496	.0314
6	19	44.10	6.9902	6.8449	-7.1355	.0326
6	20	44.60	7.0671	6.9718	-7.1624	.0333
7	2	-44.43	6.9988	6.9991	-6.9985	.0327
7	3	-44.02	6.9305	6.9685	-6.8925	.0320
7	4	-43.70	6.8102	6.8761	-6.7443	.0309
7	5	-43.50	6.6112	6.6944	-6.5280	.0291
7	6	-43.49	7.0989	7.1653	-7.0324	.0336
7	7	-43.48	11.7790	11.8687	-11.6893	.0642
7	8	-43.36	12.3523	12.5087	-12.1958	.0706
7	9	-43.43	12.2643	12.4839	-12.0447	.0696
7	10	-44.03	12.3164	12.4708	-12.1619	.0702
7	11	45.00	12.3541	12.3541	-12.3541	.0707
7	12	44.03	12.3164	12.1619	-12.4708	.0702
7	13	43.43	12.2643	12.0447	-12.4839	.0696
7	14	43.36	12.3523	12.1958	-12.5087	.0706
7	15	43.48	11.7790	11.6893	-11.8687	.0642
7	16	43.49	7.0989	7.0324	-7.1653	.0336
7	17	43.50	6.6112	6.5280	-6.6944	.0291
7	18	43.70	6.8102	6.7443	-6.8761	.0309
7	19	44.02	6.9305	6.8925	-6.9685	.0320
7	20	44.43	6.9988	6.9985	-6.9991	.0327
8	2	-44.24	6.9341	6.8475	-7.0208	.0321
8	3	-43.89	6.8848	6.8236	-6.9459	.0316
8	4	-43.72	6.7927	6.7385	-6.8470	.0308
8	5	-43.77	6.6259	6.5603	-6.6915	.0293
8	6	-43.99	7.1183	6.9894	-7.2472	.0338
8	7	-43.88	11.7880	11.6218	-11.9542	.0643
8	8	-43.45	12.3903	12.4297	-12.3509	.0711
8	9	-43.24	12.4309	12.6820	-12.1797	.0716
8	10	-43.85	12.6227	12.8308	-12.4146	.0738
8	11	-45.00	12.7166	12.7166	-12.7166	.0749
8	12	43.85	12.6227	12.4146	-12.8308	.0738
8	13	43.24	12.4309	12.1797	-12.6820	.0716
8	14	43.45	12.3903	12.3509	-12.4297	.0711
8	15	43.88	11.7880	11.9542	-11.6218	.0643
8	16	43.99	7.1183	7.2472	-6.9894	.0338
8	17	43.77	6.6259	6.6915	-6.5603	.0293
8	18	43.72	6.7927	6.8470	-6.7385	.0308
8	19	43.89	6.8848	6.9459	-6.8236	.0316
8	20	44.24	6.9341	7.0208	-6.8475	.0321
9	2	-44.05	6.8642	6.7080	-7.0204	.0314
9	3	-43.71	6.8361	6.6903	-6.9819	.0312

LISTING OF PARAMETERS (Continued)

9	4	-43.61	6.7807	6.6156	-6.9459	.0307
9	5	-43.83	6.6674	6.4513	-6.8835	.0297
9	6	-44.33	7.1670	6.7084	-7.5456	.0343
9	7	-44.17	11.8635	11.3724	-12.3546	.0652
9	8	-43.46	12.4690	12.4189	-12.5191	.0720
9	9	-43.02	12.6509	13.0660	-12.2358	.0741
9	10	-43.69	12.9349	13.2901	-12.5798	.0775
9	11	45.00	13.0844	13.0844	-13.0844	.0793
9	12	43.69	12.9349	12.5798	-13.2901	.0775
9	13	43.02	12.6509	12.2358	-13.0660	.0741
9	14	43.46	12.4690	12.5191	-12.4189	.0720
9	15	44.17	11.8635	12.3546	-11.3724	.0652
9	16	44.33	7.1670	7.5456	-6.7884	.0343
9	17	43.83	6.6674	6.8835	-6.4513	.0297
9	18	43.61	6.7807	6.9459	-6.6156	.0307
9	19	43.71	6.8361	6.9819	-6.6903	.0312
9	20	44.05	6.8642	7.0204	-6.7080	.0314
10	2	-43.95	6.7788	6.5834	-6.9741	.0306
10	3	-43.58	6.7569	6.5503	-6.9635	.0305
10	4	-43.40	6.7189	6.4499	-6.9879	.0301
10	5	-43.59	6.6472	6.2492	-7.0453	.0295
10	6	-44.25	7.0964	6.1969	-7.9959	.0339
10	7	-44.07	11.5086	10.3495	-12.6676	.0617
10	8	-43.44	11.9642	11.8153	-12.1130	.0663
10	9	-43.06	12.3375	13.3147	-11.3602	.0707
10	10	-43.82	12.8968	13.7958	-11.9979	.0772
10	11	45.00	13.1473	13.1473	-13.1473	.0800
10	12	43.82	12.8968	11.9979	-13.7958	.0772
10	13	43.06	12.3375	11.3602	-13.3147	.0707
10	14	43.44	11.9642	12.1130	-11.8153	.0663
10	15	44.07	11.5086	12.6676	-10.3495	.0617
10	16	44.25	7.0964	7.9959	-6.1969	.0339
10	17	43.59	6.6472	7.0453	-6.2492	.0295
10	18	43.40	6.7189	6.9879	-6.4499	.0301
10	19	43.58	6.7569	6.9635	-6.5503	.0305
10	20	43.95	6.7788	6.9741	-6.5834	.0306
11	2	-44.07	6.6841	6.5049	-6.8633	.0298
11	3	-43.72	6.6458	6.4451	-6.8465	.0295
11	4	-43.50	6.5904	6.3118	-6.8690	.0290
11	5	-43.58	6.5595	6.1175	-7.0016	.0288
11	6	-44.13	6.8182	5.8577	-7.7787	.0314
11	7	-44.03	7.1821	6.3846	-7.9796	.0346
11	8	-43.66	7.2705	7.1610	-7.3800	.0352
11	9	-43.53	7.7276	8.3746	-7.0806	.0400
11	10	-44.19	12.4412	13.3993	-11.4931	.0719
11	11	45.00	12.9439	12.9439	-12.9439	.0776
11	12	44.19	12.4412	11.4931	-13.3993	.0719

LISTING OF PARAMETERS (Continued)

11	13	43.53	7.7276	7.0806	-8.3746	.0400
11	14	43.66	7.2705	7.3800	-7.1610	.0352
11	15	44.03	7.1921	7.9796	-6.3846	.0346
11	16	44.13	6.8182	7.7787	-5.8577	.0314
11	17	43.58	6.5595	7.0016	-6.1175	.0288
11	18	43.50	6.5904	6.8690	-6.3118	.0290
11	19	43.72	6.6458	6.8465	-6.4451	.0295
11	20	44.07	6.6841	6.8633	-6.5049	.0298
12	2	-44.47	6.6121	6.5104	-6.7138	.0292
12	3	-44.28	6.5580	6.4483	-6.6678	.0287
12	4	-44.19	6.4848	6.3446	-6.6251	.0280
12	5	-44.32	6.4495	6.2522	-6.6467	.0277
12	6	-44.71	6.5957	6.2665	-6.9249	.0290
12	7	-44.64	6.7707	6.5191	-7.0222	.0306
12	8	-44.31	6.7951	6.7409	-6.8494	.0308
12	9	-44.12	7.3144	7.4562	-7.1726	.0357
12	10	-44.40	12.1005	12.3480	-11.8531	.0678
12	11	45.00	12.7307	12.7307	-12.7307	.0750
12	12	44.40	12.1005	11.8531	-12.3480	.0678
12	13	44.12	7.3144	7.1726	-7.4562	.0357
12	14	44.31	6.7951	6.8494	-6.7409	.0308
12	15	44.64	6.7707	7.0222	-6.5191	.0306
12	16	44.71	6.5957	6.9249	-6.2665	.0290
12	17	44.32	6.4495	6.6467	-6.2522	.0277
12	18	44.19	6.4848	6.6251	-6.3446	.0280
12	19	44.28	6.5580	6.6678	-6.4483	.0287
12	20	44.47	6.6121	6.7138	-6.5104	.0292
13	2	-45.00	6.5872	6.5872	-6.5872	.0289
13	3	-45.00	6.5306	6.5306	-6.5306	.0284
13	4	-45.00	6.4600	6.4600	-6.4600	.0278
13	5	-45.00	6.4436	6.4436	-6.4436	.0277
13	6	45.00	6.5975	6.5975	-6.5975	.0290
13	7	45.00	6.8175	6.8175	-6.8175	.0310
13	8	45.00	6.8437	6.8437	-6.8437	.0312
13	9	45.00	7.3767	7.3767	-7.3767	.0363
13	10	45.00	12.1292	12.1292	-12.1292	.0681
13	11	45.00	12.7661	12.7661	-12.7661	.0755
13	12	45.00	12.1292	12.1292	-12.1292	.0681
13	13	45.00	7.3767	7.3767	-7.3767	.0363
13	14	45.00	6.8437	6.8437	-6.8437	.0312
13	15	45.00	6.8175	6.8175	-6.8175	.0310
13	16	45.00	6.5975	6.5975	-6.5975	.0290
13	17	45.00	6.4436	6.4436	-6.4436	.0277
13	18	45.00	6.4600	6.4600	-6.4600	.0278
13	19	45.00	6.5306	6.5306	-6.5306	.0284
13	20	45.00	6.5872	6.5872	-6.5872	.0289
14	2	44.47	6.6121	6.7138	-6.5104	.0292

LISTING OF PARAMETERS (Continued)

14	3	44.28	6.5580	6.6678	-6.4483	.0287
14	4	44.19	6.4848	6.6251	-6.3446	.0280
14	5	44.32	6.4495	6.6467	-6.2522	.0277
14	6	44.71	6.5957	6.9249	-6.2665	.0290
14	7	44.64	6.7707	7.0222	-6.5191	.0306
14	8	44.31	6.7951	6.8494	-6.7409	.0308
14	9	44.12	7.3144	7.1726	-7.4562	.0357
14	10	44.40	12.1005	11.8531	-12.3480	.0678
14	11	45.00	12.7307	12.7307	-12.7307	.0750
14	12	-44.40	12.1005	12.3480	-11.8531	.0678
14	13	-44.12	7.3144	7.4562	-7.1726	.0357
14	14	-44.31	6.7951	6.7409	-6.8494	.0308
14	15	-44.64	6.7707	6.5191	-7.0222	.0306
14	16	-44.71	6.5957	6.2665	-6.9249	.0290
14	17	-44.32	6.4495	6.2522	-6.6467	.0277
14	18	-44.19	6.4848	6.3446	-6.6251	.0280
14	19	-44.28	6.5580	6.4483	-6.6678	.0287
14	20	-44.47	6.6121	6.5104	-6.7138	.0292
15	2	44.07	6.6841	6.8633	-6.5049	.0298
15	3	43.72	6.6458	6.8465	-6.4451	.0295
15	4	43.50	6.5904	6.8690	-6.3118	.0290
15	5	43.58	6.5595	7.0016	-6.1175	.0288
15	6	44.13	6.8182	7.7787	-5.8577	.0314
15	7	44.03	7.1821	7.9796	-6.3846	.0346
15	8	43.66	7.2705	7.3800	-7.1610	.0352
15	9	43.53	7.7276	7.0806	-8.3746	.0400
15	10	44.19	12.4412	11.4931	-13.3893	.0719
15	11	45.00	12.9439	12.9439	-12.9439	.0776
15	12	-44.19	12.4412	13.3893	-11.4931	.0719
15	13	-43.53	7.7276	8.3746	-7.0806	.0400
15	14	-43.66	7.2705	7.1610	-7.3800	.0352
15	15	-44.03	7.1821	6.3846	-7.9796	.0346
15	16	-44.13	6.8182	5.8577	-7.7787	.0314
15	17	-43.58	6.5595	6.1175	-7.0016	.0288
15	18	-43.50	6.5904	6.3118	-6.8690	.0290
15	19	-43.72	6.6458	6.4451	-6.8465	.0295
15	20	-44.07	6.6841	6.5049	-6.8633	.0298
16	2	43.95	6.7788	6.9741	-6.5834	.0306
16	3	43.58	6.7569	6.9635	-6.5503	.0305
16	4	43.40	6.7189	6.9879	-6.4499	.0301
16	5	43.59	6.6472	7.0453	-6.2492	.0295
16	6	44.25	7.0964	7.9959	-6.1969	.0339
16	7	44.07	11.5086	12.6676	-10.3495	.0617
16	8	43.44	11.9642	12.1130	-11.8153	.0663
16	9	43.06	12.3375	11.3602	-13.3147	.0707
16	10	43.92	12.8968	11.9979	-13.7958	.0772
16	11	45.00	13.1473	13.1473	-13.1473	.0800

LISTING OF PARAMETERS (Continued)

16	12	-43.82	12.8969	13.7958	-11.9979	.0772
16	13	-43.06	12.3375	13.3147	-11.3602	.0707
16	14	-43.44	11.9642	11.8153	-12.1130	.0663
16	15	-44.07	11.5086	10.3495	-12.6676	.0617
16	16	-44.25	7.0964	6.1969	-7.9959	.0339
16	17	-43.59	6.6472	6.2492	-7.0453	.0295
16	18	-43.40	6.7189	6.4499	-6.9879	.0301
16	19	-43.58	6.7569	6.5503	-6.9635	.0305
16	20	-43.95	6.7788	6.5834	-6.9741	.0306
17	2	44.05	6.8642	7.0204	-6.7080	.0314
17	3	43.71	6.8361	6.9819	-6.6903	.0312
17	4	43.61	6.7807	6.9459	-6.6156	.0307
17	5	43.83	6.6674	6.8835	-6.4513	.0297
17	6	44.33	7.1670	7.5456	-6.7884	.0343
17	7	44.17	11.8635	12.3546	-11.3724	.0652
17	8	43.46	12.4690	12.5191	-12.4189	.0720
17	9	43.02	12.6509	12.2358	-13.0660	.0741
17	10	43.69	12.9349	12.5798	-13.2901	.0775
17	11	-45.00	13.0844	13.0844	-13.0844	.0793
17	12	-43.69	12.9349	13.2901	-12.5798	.0775
17	13	-43.02	12.6509	13.0660	-12.2358	.0741
17	14	-43.46	12.4690	12.4189	-12.5191	.0720
17	15	-44.17	11.8635	11.3724	-12.3546	.0652
17	16	-44.33	7.1670	6.7884	-7.5456	.0343
17	17	-43.83	6.6674	6.4513	-6.8835	.0297
17	18	-43.61	6.7807	6.6156	-6.9459	.0307
17	19	-43.71	6.8361	6.6903	-6.9819	.0312
17	20	-44.05	6.8642	6.7080	-7.0204	.0314
18	2	44.24	6.9341	7.0208	-6.8475	.0321
18	3	43.89	6.8848	6.9459	-6.8236	.0316
18	4	43.72	6.7927	6.8470	-6.7385	.0308
18	5	43.77	6.6259	6.6915	-6.5603	.0293
18	6	43.99	7.1183	7.2472	-6.9894	.0338
18	7	43.88	11.7880	11.9542	-11.6218	.0643
18	8	43.45	12.3903	12.3509	-12.4297	.0711
18	9	43.24	12.4309	12.1797	-12.6820	.0716
18	10	43.85	12.6227	12.4146	-12.8308	.0738
18	11	45.00	12.7166	12.7166	-12.7166	.0749
18	12	-43.85	12.6227	12.8308	-12.4146	.0738
18	13	-43.24	12.4309	12.6820	-12.1797	.0716
18	14	-43.45	12.3903	12.4297	-12.3509	.0711
18	15	-43.88	11.7880	11.6218	-11.9542	.0643
18	16	-43.99	7.1183	6.9894	-7.2472	.0338
18	17	-43.77	6.6259	6.5603	-6.6915	.0293
18	18	-43.72	6.7927	6.7385	-6.8470	.0308
18	19	-43.89	6.8848	6.8236	-6.9459	.0316
18	20	-44.24	6.9341	6.8475	-7.0208	.0321

LISTING OF PARAMETERS (Continued)

19	2	44.43	6.9988	6.9985	-6.9991	.0327
19	3	44.02	6.9305	6.8925	-6.9685	.0320
19	4	43.70	6.8102	6.7443	-6.8761	.0309
19	5	43.50	6.6112	6.5280	-6.6944	.0291
19	6	43.49	7.0989	7.0324	-7.1653	.0336
19	7	43.48	11.7790	11.6893	-11.8687	.0642
19	8	43.36	12.3523	12.1958	-12.5087	.0706
19	9	43.43	12.2643	12.0447	-12.4839	.0696
19	10	44.03	12.3164	12.1619	-12.4708	.0702
19	11	45.00	12.3541	12.3541	-12.3541	.0707
19	12	-44.03	12.3164	12.4708	-12.1619	.0702
19	13	-43.43	12.2643	12.4939	-12.0447	.0696
19	14	-43.36	12.3523	12.5087	-12.1958	.0706
19	15	-43.48	11.7790	11.8687	-11.6893	.0642
19	16	-43.49	7.0989	7.1653	-7.0324	.0336
19	17	-43.50	6.6112	6.6944	-6.5280	.0291
19	18	-43.70	6.8102	6.8761	-6.7443	.0309
19	19	-44.02	6.9305	6.9685	-6.8925	.0320
19	20	-44.43	6.9988	6.9991	-6.9985	.0327
20	2	44.60	7.0671	6.9718	-7.1624	.0333
20	3	44.10	6.9902	6.8449	-7.1355	.0326
20	4	43.59	6.8559	6.6622	-7.0496	.0314
20	5	43.12	6.6391	6.4025	-6.8757	.0294
20	6	42.92	7.1130	6.8652	-7.3607	.0338
20	7	43.03	11.7754	11.4431	-12.1077	.0642
20	8	43.17	12.2941	11.9904	-12.5977	.0700
20	9	43.47	12.1068	11.8423	-12.3714	.0679
20	10	44.12	12.0579	11.9015	-12.2143	.0673
20	11	-45.00	12.0547	12.0547	-12.0547	.0673
20	12	-44.12	12.0579	12.2143	-11.9015	.0673
20	13	-43.47	12.1068	12.3714	-11.8423	.0679
20	14	-43.17	12.2941	12.5977	-11.9904	.0700
20	15	-43.03	11.7754	12.1077	-11.4431	.0642
20	16	-42.92	7.1130	7.3607	-6.8652	.0338
20	17	-43.12	6.6391	6.8757	-6.4025	.0294
20	18	-43.59	6.8559	7.0496	-6.6622	.0314
20	19	-44.10	6.9902	7.1355	-6.8449	.0326
20	20	-44.60	7.0671	7.1624	-6.9718	.0333
21	2	44.77	7.1424	6.9520	-7.3327	.0340
21	3	44.16	7.0692	6.8140	-7.3244	.0333
21	4	43.46	6.9362	6.6084	-7.2640	.0321
21	5	42.70	6.7122	6.3106	-7.1139	.0301
21	6	42.30	7.1580	6.7118	-7.6041	.0342
21	7	42.51	11.7653	11.1414	-12.3691	.0642
21	8	42.90	12.2079	11.7209	-12.6949	.0691
21	9	43.42	11.9547	11.5960	-12.3134	.0662
21	10	44.15	11.8509	11.6599	-12.0428	.0650

LISTING OF PARAMETERS (Continued)

21	11	-45.00	11.8262	11.8262	-11.8262	.0647
21	12	-44.15	11.8509	12.0428	-11.6590	.0650
21	13	-43.42	11.9547	12.3154	-11.5960	.0662
21	14	-42.90	12.2079	12.6949	-11.7209	.0691
21	15	-42.51	11.7653	12.3691	-11.1614	.0642
21	16	-42.30	7.1580	7.6041	-6.7118	.0342
21	17	-42.70	6.7122	7.1139	-6.3106	.0301
21	18	-43.46	6.9362	7.2640	-6.6084	.0321
21	19	-44.16	7.0692	7.3244	-6.8140	.0333
21	20	-44.77	7.1424	7.3327	-6.9520	.0340
22	2	44.93	7.2208	6.9447	-7.4968	.0348
22	3	44.24	7.1615	6.8004	-7.5226	.0342
22	4	43.36	7.0457	6.5799	-7.5114	.0332
22	5	42.29	6.8305	6.2461	-7.4150	.0312
22	6	41.60	7.2351	6.5402	-7.9299	.0351
22	7	41.92	11.7434	10.7966	-12.6901	.0641
22	8	42.62	12.0959	11.3818	-12.8100	.0679
22	9	43.37	11.8187	11.3301	-12.3074	.0647
22	10	44.18	11.7057	11.4565	-11.9548	.0635
22	11	-45.00	11.6776	11.6776	-11.6776	.0631
22	12	-44.18	11.7057	11.9548	-11.4565	.0635
22	13	-43.37	11.8187	12.3074	-11.3301	.0647
22	14	-42.62	12.0959	12.8100	-11.3818	.0679
22	15	-41.92	11.7434	12.6901	-10.7966	.0641
22	16	-41.60	7.2351	7.9299	-6.5402	.0351
22	17	-42.29	6.8305	7.4150	-6.2461	.0312
22	18	-43.36	7.0457	7.5114	-6.5799	.0332
22	19	-44.24	7.1615	7.5226	-6.8004	.0342
22	20	-44.93	7.2208	7.4968	-6.9447	.0348
23	2	-44.97	7.2904	6.9511	-7.6298	.0355
23	3	44.32	7.2454	6.7923	-7.6985	.0351
23	4	43.35	7.1605	6.5591	-7.7618	.0343
23	5	41.99	6.9854	6.1991	-7.7718	.0328
23	6	40.84	7.3470	6.3041	-8.3900	.0364
23	7	41.29	11.7045	10.2862	-13.1229	.0640
23	8	42.45	11.9684	10.9798	-12.9570	.0666
23	9	43.43	11.7291	11.0831	-12.3750	.0638
23	10	44.26	11.6495	11.3292	-11.9699	.0629
23	11	-45.00	11.6323	11.6323	-11.6323	.0626
23	12	-44.26	11.6495	11.9699	-11.3292	.0629
23	13	-43.43	11.7291	12.3750	-11.0831	.0638
23	14	-42.45	11.9684	12.9570	-10.9798	.0664
23	15	-41.29	11.7045	13.1229	-10.2862	.0640
23	16	-40.84	7.3470	8.3900	-6.3041	.0364
23	17	-41.99	6.9854	7.7718	-6.1991	.0328
23	18	-43.35	7.1605	7.7619	-6.5591	.0343
23	19	-44.32	7.2454	7.6985	-6.7923	.0351
23	20	44.97	7.2904	7.6298	-6.9511	.0355

LISTING OF PARAMETERS (Continued)

24	2	44.94	7.3283	6.9662	-7.6904	.0359
24	3	44.30	7.2785	6.7639	-7.7931	.0354
24	4	43.44	7.2225	6.4973	-7.9477	.0350
24	5	42.00	7.1252	6.1308	-8.1195	.0342
24	6	40.16	7.4837	5.9084	-9.0590	.0383
24	7	40.81	11.6781	9.5696	-13.7867	.0644
24	8	42.58	11.8874	10.5857	-13.1891	.0659
24	9	43.66	11.7491	10.9286	-12.5696	.0641
24	10	44.40	11.7199	11.3242	-12.1157	.0636
24	11	-45.00	11.7154	11.7154	-11.7154	.0635
24	12	-44.40	11.7199	12.1157	-11.3242	.0636
24	13	-43.66	11.7491	12.5696	-10.9286	.0641
24	14	-42.58	11.8874	13.1891	-10.5857	.0659
24	15	-40.81	11.6781	13.7867	-9.5696	.0644
24	16	-40.16	7.4837	9.0590	-5.9084	.0383
24	17	-42.00	7.1252	8.1195	-6.1308	.0342
24	18	-43.44	7.2225	7.9477	-6.4973	.0350
24	19	-44.30	7.2785	7.7931	-6.7639	.0354
24	20	-44.94	7.3283	7.6904	-6.9662	.0359

BIBLIOGRAPHY

Bollinger, G. A. (1973). Seismicity and crustal uplift in the southeastern United States. Am. J. Sei., Cooper, vol. 273-A, pp. 396-408.

Bridge, S. R. (1975). Evaluation of Stress Drop of the August 2, 1974 Georgia-South Carolina Earthquake and Aftershock Sequence, Georgia Institute of Technology.

Byerlee, J. D., and W. F. Brace (1960. Stick-slip stable sliding and earthquakes-effect of rock type, pressure, strain rate and stiffness. J. Geophys. Res., 73(18) pp. 6031-6037.

Byerlee, J. S., and W. F. Brace (1972). Fault stability and pore pressure. Bull, Seismol. Sco. Am., 62(2), pp. 657-660.

Champin, J. W., Jr. (1975). Bouguer Gravity Map of the Summerville-Charleston, South Carolina Epicentral Zone and Tectonic Implications. Georgia Institute of Technology.

Denman, H. E. (1974) Implications of Seismic Activity at the Clark Hill Reservior. Georgia Institute of Technology.

Dieterich, J. H. (1969). Mathematical modeling of fault zone tectonics and seismicity. Abstracts of Geol. Soc. Amer., Annual Meeting at Atlantic City, N. J., part 7, pp. 47-48.

Griggs, D. T., and D. W. Baker (1969). The origin of deep focus earthquakes. In: H. Mark and S. Fenback (Editors), Properties of Matter under unusual Conditions, Interscience Publishers, N. Y., pp23-42.

Ide, J. M. (1936). The elastic properties of rocks: a correlation of theory and experiment. Proc. Natl. Acad. Sci. U. S., 22, p. 482.

Jeffereys, H. (1936). Note on fracture. Roy. Soc. Edinburg Proc., 56, pp. 158-163.

Knopoff, L. (1964). Earth tide as a triggering mechanism for earthquakes. B.S.S.A. 54(6), pp. 1865-1870.

Lister, C.R.B. (1974). On the penetration of water into hot rock. Geophys. J. R. Astro. Soc., 39, pp 465-509.

Long, L.T., H.E. Denman, H. Yung-An Hsiao and G.E. Marion (1976). Gravity and seismic studies in the Clark Hill Reservior Area. Stratigraphy, Structure, and Seismicity in Slate Belt Rocks Along the Savannah River, Guidebook 16, Georgia Geological Society, Atlanta, 1976, pp. 33-41.

BIBLIOGRAPHY
(Continued)

Long, L.T. and H. Yung-An Hsiao (1976). The stress amplification mechanism for intraplate eqrthquakes applied to Southeast United States, The Geological Society of America, "Abstracts with Programs", V, 8 (2), February, 1976, Boulder, Colorado.

Long, L.T. (1976). Speculations concerning southeastern earthquakes, mafic intrusions, gravity anomalies, and stress amplification, Earthquake Notes, V. 47,(3), July-September 1976.

Long, L.T. (1975). A Study of Microearthquakes in the Southeastern United States, Georgia Institute of Technology.

Marion, G.E. (1977). A Spectral Analysis of Microearthquakes, That Occur in the Southeastern United States. Georgia Institute of Technology.

Mckee, J.H. (1974). A Geophysical Study of Microearthquake Activity Near Bowman, South Carolina. Georgia Institute of Technology.

Nafe and Drake (unpublished), (1959) In: a crust section across the Puerto Rico Trech. J. Geophys. Res., 64 (10), p. 1548.

Orowan, E. (1960). Mechanism of Seismic faulting. In: Rock Deformation, Geol. Soc. Amer. Mem., 79, pp. 323-345

Ramberg, H. (1967). Gravity, Deformation and the Earth's Crust. Academic Press, Inc., N.Y.

Reid, H.F. (1911). The Mechanisms of the Earthquake, The California Earthquake of April 18, 1906, Report of the State Investigation Commission, Vol. 2, Carnegie Institution of Washington, Washington, D. C., 1910.

Talwani, P. (1976) Earthquakes associated with the Clark Hill Reservior, South Carolina-A case of induced seismicity. In: W. G. Milne (Editor), Induced Seismicity. Eng. Geol. 10(2-4) pp. 239-253.

Timoshenko, S. P., and J. N. Goodier (1970). The Theory of Elasticity. McGraw-Hill Book Company.

Woolard, G. P. (1959). Crustal structure from gravity and seismic measurements, J. Geophys. Res. 64, pp. 1521-1544.

Zisman, W. A. (1933). Comparison of the statically and seismologically determined elastic constants of rocks. Proc. Natl. Acad. Sci. U.S., 19,680.